

DUDLEY KNOX LIBRARY
NAVAL POSTGRADUATE SCHOOL
MONTEREY CA 93943-5101

Approved for public release; distribution is unlimited.

**Use of Minimum Time Controllers in Vertically-Launched
Surface-to-Air Missiles**

by

Timothy Brian Mull
Lieutenant, United States Navy
B.S., University of Idaho, 1984

Submitted in partial fulfillment of the requirements for
the degree of

**MASTER OF SCIENCE IN ELECTRICAL
ENGINEERING**

from the

NAVAL POSTGRADUATE SCHOOL
June 1992

— 1 —

REPORT DOCUMENTATION PAGE				Form Approved OMB No. 0704-0188	
REPORT SECURITY CLASSIFICATION Unclassified			1b. RESTRICTIVE MARKINGS		
SECURITY CLASSIFICATION AUTHORITY			3. DISTRIBUTION/AVAILABILITY OF REPORT Approved for public release distribution unlimited.		
DECLASSIFICATION/DOWNGRADING SCHEDULE					
PERFORMING ORGANIZATION REPORT NUMBER(S)			5. MONITORING ORGANIZATION REPORT NUMBER(S)		
NAME OF PERFORMING ORGANIZATION Naval Postgraduate School		6b. OFFICE SYMBOL (If applicable) Code 33	7a. NAME OF MONITORING ORGANIZATION Naval Postgraduate School		
ADDRESS (City, State, and ZIP Code) Monterey, CA 93943-5000			7b. ADDRESS (City, State, and ZIP Code) Monterey, CA 93943-5000		
NAME OF FUNDING/SPONSORING ORGANIZATION		8b. OFFICE SYMBOL (If applicable)	9. PROCUREMENT INSTRUMENT IDENTIFICATION NUMBER		
ADDRESS (City, State, and ZIP Code)		10. SOURCE OF FUNDING NUMBERS			
		PROGRAM ELEMENT NO.	PROJECT NO.	TASK NO.	WORK UNIT ACCESSION NO.

TITLE (Include Security Classification)
USE OF MINIMUM TIME CONTROLLERS IN VERTICALLY-LAUNCHED SURFACE-TO-AIR MISSILES

PERSONAL AUTHOR(S)
Timothy Brian Mull

1. TYPE OF REPORT Master's Thesis	13b. TIME COVERED FROM _____ TO _____	14. DATE OF REPORT (Year,Month,Day) June 1992	15. PAGE COUNT 78
--------------------------------------	--	--	----------------------

SUPPLEMENTARY NOTATION
The views expressed in this thesis are those of the author and do not reflect the official policy or position of the Department of Defense or the U.S. Government.

COSATI CODES			18. SUBJECT TERMS (Continue on reverse if necessary and identify by block number) Missile Guidance, Pontryagin's Minimum Principle, Bang-Bang Controllers.
FIELD	GROUP	SUB-GROUP	

ABSTRACT (Continue on reverse if necessary and identify by block number)
This thesis develops the concept of minimum-time (Bang-Bang) controllers and their application to missile control. Based on Pontryagin's minimum principle, a minimum-time second order controller is derived. This controller is then applied to control of a vertically-launched surface-to-air missile. In the boost phase of missile flight, the minimum-time controller drives the missile body axis from vertical to a commanded angle in minimum time. In the terminal phase of the missile-target engagement, the minimum-time controller drives the time rate of change of the line of sight angle to zero in minimum time. The results obtained with the minimum time controller are compared with those obtained with the Proportional Navigation control algorithm, which is commonly used in tactical surface-to-air and air-to-air missile.

. DISTRIBUTION/AVAILABILITY OF ABSTRACT <input checked="" type="checkbox"/> UNCLASSIFIED/UNLIMITED <input type="checkbox"/> SAME AS RPT. <input type="checkbox"/> DTIC USERS		21. ABSTRACT SECURITY CLASSIFICATION Unclassified	
a. NAME OF RESPONSIBLE INDIVIDUAL Harold A. Titus		22b. TELEPHONE (Include Area Code) (408) 646 - 2560	22c. OFFICE SYMBOL EC/Ts

ABSTRACT

This thesis develops the concept of minimum-time (Bang-Bang) controllers and their application to missile control. Based on Pontryagin's minimum principle, a minimum-time second order controller is derived. This controller is then applied to control of a vertically-launched surface-to-air missile. In the boost phase of missile flight, the minimum-time controller drives the missile body axis from vertical to a commanded angle in minimum time. In the terminal phase of the missile-target engagement, the minimum-time controller drives the time rate of change of the line of sight angle to zero in minimum time. The results obtained with the minimum time controller are compared with those obtained with the Proportional Navigation control algorithm, which is commonly used in tactical surface-to-air and air-to-air missile.

M8877
C.1

DISCLAIMER

The reader is cautioned that computer programs developed in this research may not have been exercised for all cases of interest. While every effort has been made, within the time available, to ensure that the programs are free of computational and logical errors, they cannot be considered validated. Any application of these programs without additional verification is at the risk of the user.

Table of contents

- I. INTRODUCTION 1**
- II. CONCEPT OF BANG-BANG CONTROL..... 3**
 - A. PONTRYAGIN'S MINIMUM PRINCIPLE..... 3
 - B. APPLICATION TO A SECOND ORDER SYSTEM.....5
- III. DEVELOPMENT OF EQUATIONS OF MOTION FOR A
VERTICALLY-LAUNCHED MISSILE..... 11**
 - A. BOOST PHASE CONTROLLER..... 15
 - B. TERMINAL PHASE 18
 - 1. Missile-Target Geometry..... 18
 - 2. Missile Guidance Laws..... 21
 - a. Proportional Navigation Control.....2 2
 - b. Bang-Bang Control Minimizing Line-of-
Sight Rate.....2 8
 - 3. Missile Dynamics..... 28
- IV. VERTICAL LAUNCH MISSILE BOOST PHASE
SIMULATION..... 30**
 - A. OVERVIEW 30
 - B. MISSILE PARAMETERS..... 30
 - C. CANNISTER EGRESS..... 31
 - D. BOOST SIMULATION AND RESULTS..... 31
- V. TERMINAL PHASE SIMULATIONS..... 36**
 - A. CASE ONE 36
 - B. CASE TWO 42
- VI. CONCLUSIONS AND RECOMMENDATIONS..... 47**
- APPENDIX 1- BOOST PHASE MATLAB PROGRAM..... 48**
- APPENDIX 2- TERMINAL PHASE MATLAB PROGRAM..... 55**
- REFERENCES 68**
- INITIAL DISTRIBUTION LIST..... 69**

List of Figures

Figure 1.	Anti-ship cruise missile terminal maneuver	1
Figure 2.	Trajectories for $u=-N$	7
Figure 3.	Trajectories for $u=+N$	8
Figure 4.	Optimal switching curves.....	9
Figure 5.	Optimal control switching schemes	10
Figure 6.	Forces acting on a missile in flight.....	13
Figure 7.	Boost Phase Diagram.....	16
Figure 8.	Bang-Bang Control Law with Linear Zone.....	17
Figure 9.	Missile-target geometry	18
Figure 10.	Luenberger Observer for estimating $\dot{\sigma}$ and $\ddot{\sigma}$	21
Figure 11.	Constant Line-of-Sight Intercept.....	22
Figure 12.	Vectorial Proportional Navigation Scheme.....	24
Figure 13.	Missile Acceleration Orientation	25
Figure 14.	Missile Acceleration Relationship.....	26
Figure 15.	Missile Dynamics.....	29
Figure 16.	Missile Boost Phase Trajectories.....	32
Figure 17.	Missile Boost Phase Velocity Magnitude Profiles.....	33
Figure 18.	Missile Boost Phase Angle of Attack Profiles.....	34
Figure 19.	Missile Boost Phase Pitch Angle Profiles.....	35
Figure 20.	Case One: Missile/Target trajectories using true line of sight rate.....	37
Figure 21.	Case One: Control force versus time using proportional navigation control with true line of sight rate.....	38
Figure 22.	Case One: Control force versus time using Bang-Bang control with true line of sight rate.....	39
Figure 23.	Case One: Missile/Target trajectories using estimated values for line of sight rate.....	39
Figure 24.	Case One: Control force versus time using proportional navigation control with estimated values for line of sight rate.....	40
Figure 25.	Case One: Control force versus time using Bang-Bang control with estimated values for line of sight rate.....	40
Figure 26.	Case One: Missile/Target trajectories using Bang-Bang control, comparing true and estimated values for line of sight rate	41

Figure 27. Case Two: Missile/Target trajectories using true line of sight rate..... 43

Figure 28. Case Two: Control force versus time using Proportional Navigation control with true line of sight rate..... 44

Figure 29. Case Two: Control force versus time using Bang-Bang control with true line of sight rate..... 44

Figure 30. Case Two: Missile/Target trajectories using estimated values for line of sight rate..... 45

Figure 31. Case Two: Control force versus time using proportional navigation control with estimated values for line of sight rate..... 46

Figure 32. Case Two: Control force versus time using Bang-Bang control with estimated values for line of sight rate..... 46

ACKNOWLEDGMENTS

I wish to thank Professor Hal Titus for his ceaseless support and assistance, without which this thesis would not have been completed. His commitment to the students of the Naval Postgraduate School is unquestionable.

I would also like to thank Colin Cooper for all his assistance in the computer simulations.

Finally, the support and encouragement of my wife enabled me to devote the countless hours required to complete this thesis. Thank you, Patrice.

I. INTRODUCTION

In modern missile warfare, new technologies are producing faster, more accurate anti-ship cruise missiles (ASCM). They are able to fly at very low altitudes and perform a high speed 'pop-up' maneuver just before impact, in order to defeat the ship's missile defenses, as shown in Figure 1. In order to counter the advanced ASCM's, new control schemes must be developed to

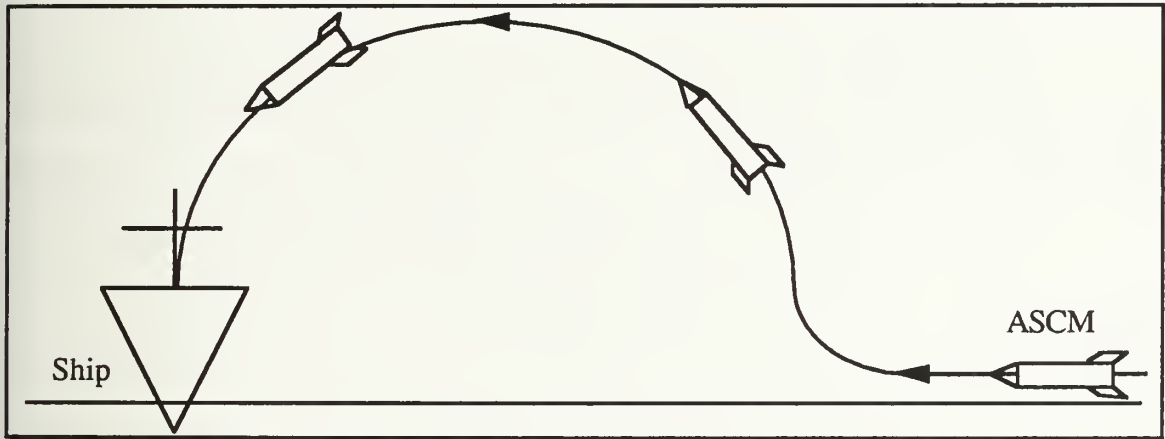


Figure 1. Anti-ship cruise missile terminal maneuver

enable the ship's surface-to-air missiles to counter this threat.

The aim of this thesis is to illustrate the concept of Bang-Bang control and how it applies to control of vertically-launched surface-to-air missiles. Bang-Bang control can be used in the missile boost phase in order to turn the missile downrange in minimum time, and also in the terminal phase, where the missile must react very quickly in order to intercept a maneuvering target.

This work applies the minimum-time (Bang-Bang) control concept to vertically-launched surface-to-air missiles. In Chapter II, the concept of

control is defined and solved for a second order system. In Chapter III, the equations of motion for a vertically-launched missile in the boost and terminal phases are developed. In Chapter IV, the boost simulations comparing missile trajectory versus maximum thrust vector control (TVC) angle are presented. In Chapter V, the terminal phase missile simulations are presented for a non-maneuvering target and also for a maneuvering target.

II. CONCEPT OF BANG-BANG CONTROL

In this section the form of the optimal control for a particular class of systems will be determined by using Pontryagin's Minimum Principle.

A. PONTYAGIN'S MINIMUM PRINCIPLE

It shall be assumed that the state equations of the system are of the form

$$\dot{\mathbf{x}} = \mathbf{Ax} + \mathbf{Bu}, \quad (2-1)$$

where \mathbf{A} is an n by n array, \mathbf{B} is an n by m array, and \mathbf{A} and \mathbf{B} may be explicitly dependent on the states and time. For this research it will be assumed that there is a single input; therefore, m is 1. It is specified that the admissible controls must satisfy the inequality constraints

$$N_- \leq u(t) \leq N_+ \quad (2-2)$$

where N_- and N_+ are the known lower and upper bounds for the control input. It is desired to drive \mathbf{x} from an initial state $\mathbf{x}(t_0)$ to a desired final state $\mathbf{x}(t_f)$, where t_0 is the problem start time and t_f is the problem end. The optimal control is that control which drives the state from its initial state to desired final state using the least "cost". The cost can be any desired measure of system performance. In the case of a minimum-time controller, the cost function can be represented as

$$J = \int_{t_0}^{t_f} dt = t_f - t_0. \quad (2-3)$$

Pontryagin's Minimum Principle states that the optimal control, u^* , which minimizes the cost function, must minimize the Hamiltonian, which is defined as

$$H(x(t), u(t), p(t), t) = 1 + p^T(t)(Ax(t) + Bu(t)) \quad (2-4)$$

where $p(t)$ is a Lagrange multiplier vector, and is arbitrary. $p(t)$ can be defined as the 'costates' of the system, and $p(t)$ can be written as

$$p(t) = \begin{bmatrix} p_1(t) \\ p_2(t) \end{bmatrix}. \quad (2-5)$$

The necessary condition for the optimal control u^* to minimize the cost function J is

$$H(x^*(t), u^*(t), p^*(t), t) \leq H(x^*(t), u(t), p^*(t), t) \quad (2-6)$$

for all times between t_0 and t_f and for all admissible controls. The asterisks in equation (2-6) represent the optimum values, and thus,

$$1 + p^{*T}(t)Ax^*(t) + p^{*T}(t)Bu^*(t) \geq 1 + p^{*T}(t)Ax^*(t) + p^{*T}(t)Bu(t) \quad (2-7)$$

Therefore

$$p^{*T}(t)Bu^*(t) \leq p^{*T}(t)Bu(t) \quad (2-8)$$

for all admissible $u(t)$ and for all times from t_{initial} to t_{final} . If $u(t)$ is constrained to $\pm N$, the optimal control $U^*(t)$ is

$$u^*(t) = \begin{cases} -N & \text{for } p_2^* > 0 \\ +N & \text{for } p_2^* < 0 \end{cases} \triangleq -N \text{sign}(p_2^*) \quad (2-9)$$

This indicates that the time-optimal control is 'Bang-Bang'; that is, the optimum control switches between its maximum positive and negative values. There are also three ideas which deserve mention:

(1) (Existence)

If all the eigenvalues of A have nonpositive real parts, then an optimal control exists that transfers any initial state x_0 to the origin. If there are positive eigenvalues (i.e. unstable roots), there may be some region of the state space where the system is uncontrollable.

(2) (Uniqueness)

If an optimal control exists, then it is unique.

(3) (Number of Switchings)

If the eigenvalues of A are all real, and a (unique) time-optimal control exists, then the control can switch at most $(n-1)$ times.

Thus, an n th-order system having all real, non-positive eigenvalues has a unique time-optimal control that switches at most $n-1$ times (not counting switching off at time t_{final}). For complex conjugate eigenvalues, more than $n-1$ switchings may be required.[1]

B. APPLICATION TO A SECOND ORDER SYSTEM

In order to illustrate the minimum principle, consider the second order differential equation

$$\ddot{x} = u, \quad (2-10)$$

or in state space,

$$\begin{bmatrix} \dot{x}_1 \\ \dot{x}_2 \end{bmatrix} = \begin{bmatrix} 0 & 1 \\ 0 & 0 \end{bmatrix} \begin{bmatrix} x_1 \\ x_2 \end{bmatrix} + \begin{bmatrix} 0 \\ 1 \end{bmatrix} u. \quad (2-11)$$

From the minimum principle, the time-optimal control for this system is $\pm N$. Thus the segment of optimal trajectories can be found by integrating the state equations (2-11), with $u=\pm N$, from time t_0 to t . This yields the results

$$x_2(t) = \pm N t + C_1 \quad (2-12)$$

$$x_1(t) = \pm N \frac{t^2}{2} + C_1 t + C_2 \quad (2-13)$$

where

$$C_1 = \mp N t_0 + x_2(t_0) \quad (2-14)$$

and

$$C_2 = \mp N \frac{t_0^2}{2} - C_1 t_0 + x_1(t_0). \quad (2-15)$$

C_1 and C_2 are functions of the initial conditions and can be treated as constants. Time can be eliminated from equations (2-12) and (2-13) by squaring the first equation, dividing the result by $2N$, and comparing the result with equation (2-13) to obtain

$$x_1(t) = \frac{1}{2N} x_2^2(t) + C_3 \quad \text{for } U = +N \quad (2-16)$$

$$x_1(t) = -\frac{1}{2N} x_2^2(t) + C_4 \quad \text{for } U = -N \quad (2-17)$$

where

$$C_3 = C_2 - \frac{C_1}{2N} \quad (2-18)$$

$$C_4 = C_2 + \frac{C_1}{2N} \quad (2-19)$$

C_3 and C_4 are functions of the initial conditions and may also be treated as constants. Equations (2-18) and (2-19) each define a family of parabolas, as shown in Figures 2 and 3.

Analysis of Figures 2 and 3 reveal the controls corresponding to the following situations:

1. $u^*=+1$ implies that the initial state x_0 lies on segment AO at time t_0 .
2. $u^*=-1$ implies that the initial state x_0 lies on segment BO at time t_0 .

This defines the optimal control to reach the origin. In order to reach these zero trajectories, the opposite value of control is required. It can be seen from

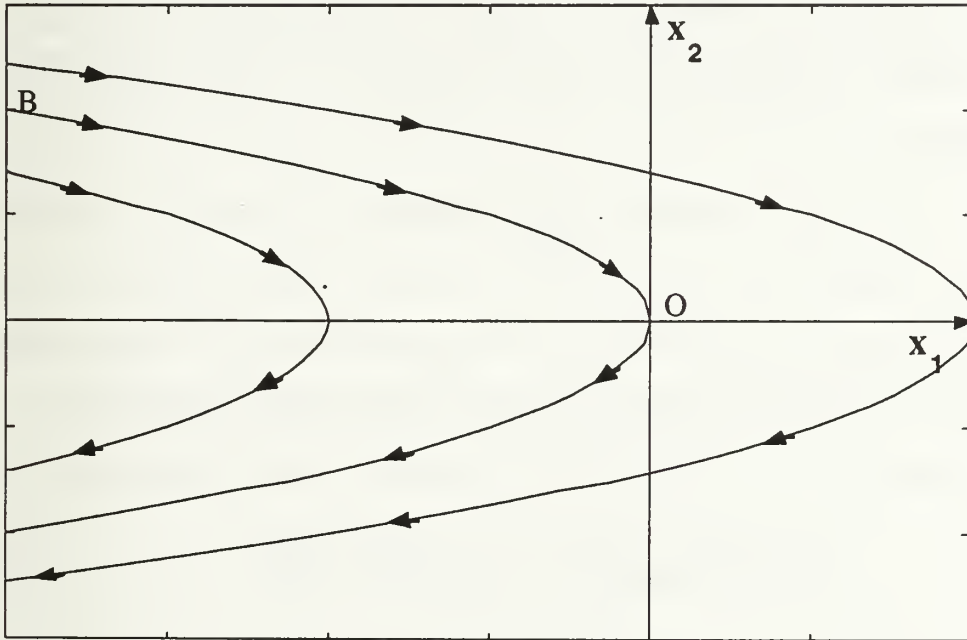


Figure 2. Trajectories for $u=-N$

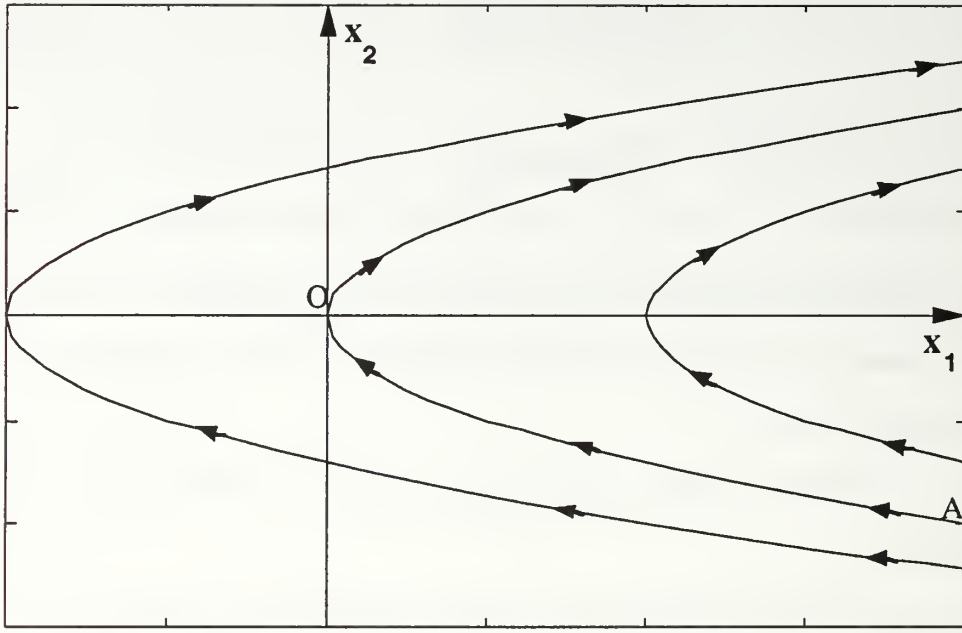


Figure 3. Trajectories for $u=+N$

Figure 4 that the two segments AO and BO form a single curve. This curve is known as the switching curve. All states that fall above the switching curves will result in the control input $U=-N$, and those states which fall below the switching curves will result in the control input $U=+N$. This curve can be represented as

$$x_1(t) = -\frac{1}{2N} x_2(t) |x_2(t)| \quad (2-20)$$

Thus, the control law can be obtained by moving all the terms of equation (2-20) to one side:

$$U(t) = -N \text{sign} \left(x_1(t) + \frac{1}{2N} x_2(t) |x_2(t)| \right) \quad (2-21)$$

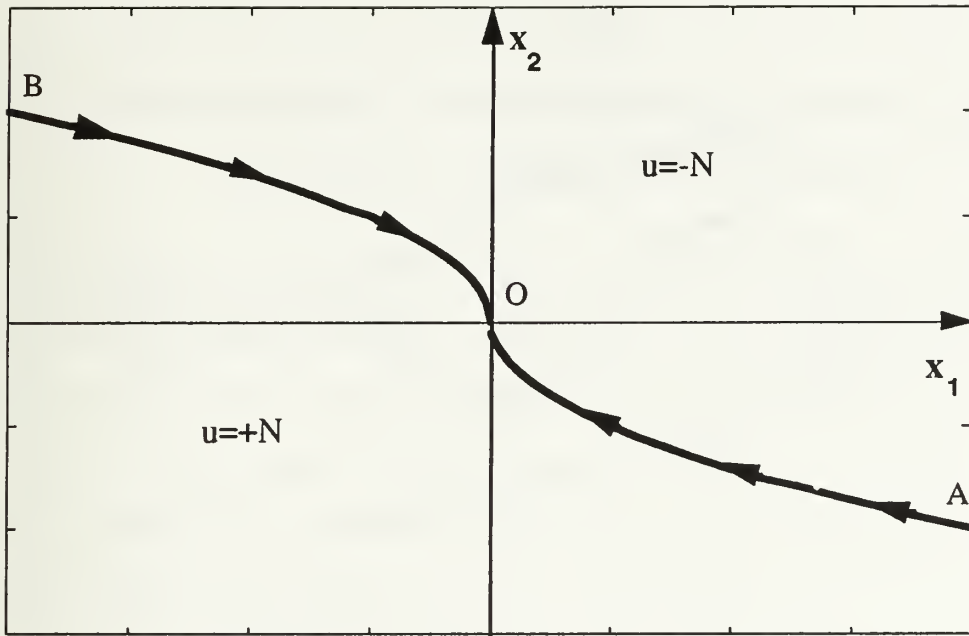


Figure 4. Optimal switching curves

Examples of the use of this switching law is shown in Figure 5. From any arbitrary initial state, the trajectory will follow the parabola that passes through the start point until the trajectory reaches the optimal switching curve. Then the control switches signs, and follows the optimum parabolic path to the origin.

Equation (2-21) is the mathematical representation of the Bang-Bang control law. This control law can be used in numerous applications where it is desired to transfer a state from initial conditions to desired final conditions in minimum time. Two examples that are of interest in this research are:

1) drive a state, such as a position, to zero in minimum time. The control law for this portion of the missile flight is of the form

$$U(t) = -N \text{sign} \left(x_1(t) + \frac{1}{2N} x_2(t) |x_2(t)| \right), \quad (2-22)$$

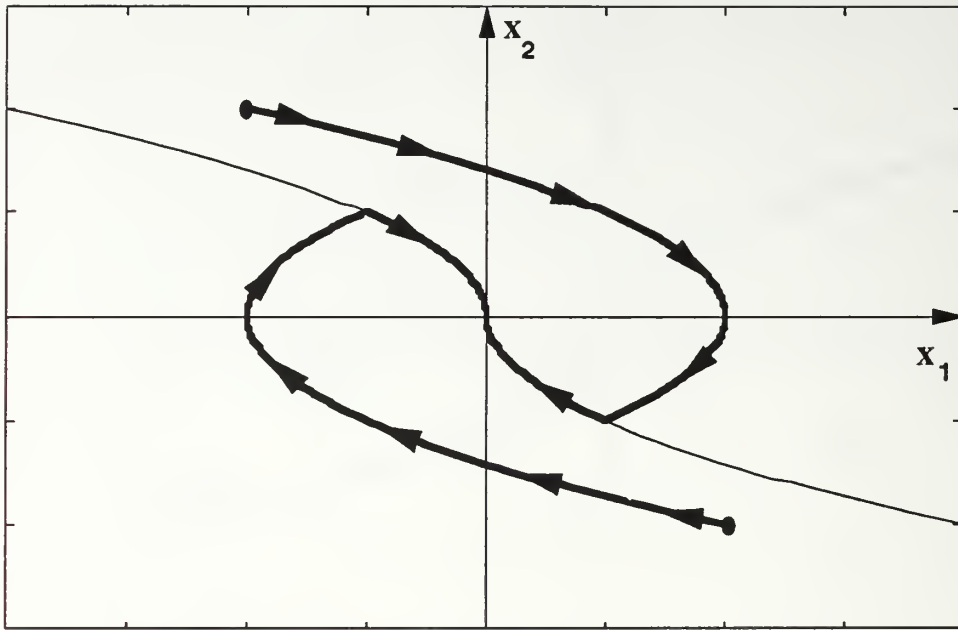


Figure 5. Optimal control switching schemes

where $x_1(t)$ is the position at time t , $x_2(t)$ is the velocity at time t , and N is the maximum admissible force that can be used to accelerate or decelerate the state; and

2) drive the time rate of change of a state to zero. In this case it is desired to keep a state constant, as opposed to driving it to zero. The form of the controller is also given by equation (2-22), but x_1 in this case will represent velocity and x_2 will represent acceleration, with N being the maximum admissible control with which to change the states.

In the next chapter, the application of the second order Bang-Bang controller to boost phase and terminal phase missile control will be examined.

III. DEVELOPMENT OF EQUATIONS OF MOTION FOR A VERTICALLY-LAUNCHED MISSILE

The equations of motion for a missile can be derived from Newton's second law of motion, which states that the summation of all external forces acting on a body must be equal to the time rate of change of its momentum, and the summation of the external moments acting on a body must be equal to the time rate of change of its moment of momentum (angular momentum). The time rates of change can be expressed by two vector equations:

$$\sum \mathbf{F}_i = \frac{d}{dt} (m \mathbf{V}_T)_i \quad (3-1)$$

and

$$\sum \mathbf{M}_i = \frac{d\mathbf{H}_i}{dt} \quad (3-2)$$

where i indicates i^{th} cartesian coordinate of the vector with respect to inertial space. By definition, \mathbf{H} is the angular momentum, or moment of momentum, of a revolving body.[2]

There are several assumptions that are made in order to simplify the problem:

1. The mass of the missile remains constant.
2. The missile airframe is a rigid body.
3. The earth is an inertial reference, and unless otherwise stated, the atmosphere is fixed with respect to earth.

In order to completely describe the motion of a missile in three dimensions, a total of six nonlinear differential equations must be solved. However, certain assumptions will be made in order to reduce the number of equations needed to adequately describe the motion of the missile:

1. The X axis will be assumed to be downrange from the launch platform to the target, the Y axis will be crossrange, and the Z axis will be altitude.

2. The type of missile studied here is known as a skid-to-turn missile, as this missile uses direct side force to turn. Thus, there will be no coupling terms between the pitch and yaw axes, and one set of equations will describe the motion in each of the Y and Z planes.

3. It will be assumed that the missile is roll stabilized, i.e., that there will be no turning moments about the X axis.

4. Since there are no cross-coupling terms between the pitch and yaw axes, the simulation can be broken into two problems, one where the pitch angle is held constant, and the other where the yaw angle is held constant. In this discussion the yaw angle will be assumed to be constant at zero. Using these assumptions, a 3 degree-of-freedom model can be developed. The force diagram of a 3 DOF missile in flight is shown in Figure 6. The governing equations of motion of this missile are:

$$\sum F_x = m\ddot{x} = -F_{\text{lift}} \sin \gamma_m + T \cos(\theta_m + \delta) - F_{\text{drag}} \cos \gamma_m \quad (3-3)$$

$$\sum F_z = m\ddot{z} = -mg + F_{\text{lift}} \cos \gamma_m + T \sin(\theta_m + \delta) - F_{\text{drag}} \sin \gamma_m \quad (3-4)$$

$$\sum M_{cg} = I_{cg} \ddot{\theta} = -F_{\text{lift}} L_{pg} \cos \gamma_m - F_{\text{drag}} L_{pg} \sin \gamma_m - TL_{tg} \sin \delta \quad (3-5)$$

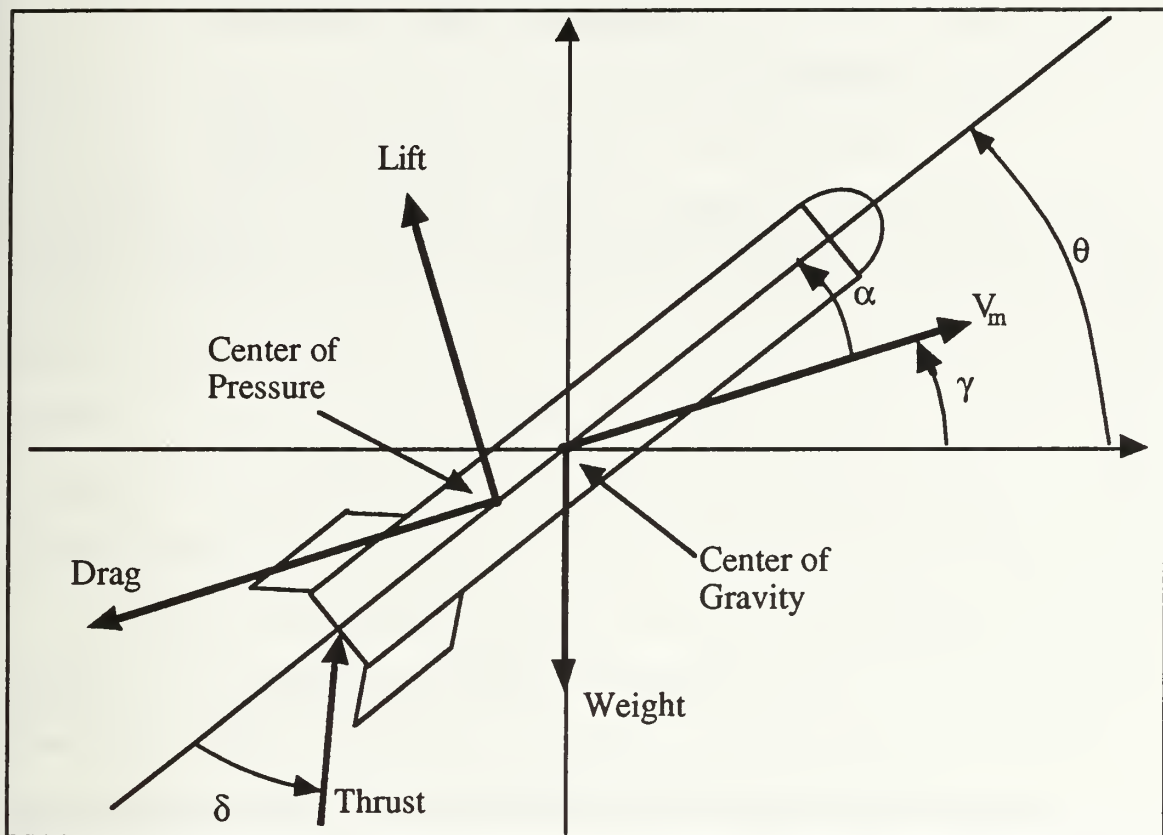


Figure 6. Forces acting on a missile in flight

where:

m missile mass (Kg)

g gravity (9.81 m/s^2)

F_{lift} aerodynamic lift force (N)

F_{drag} aerodynamic drag force (N)

γ_m angle of velocity vector from reference

θ_m angle of missile head from reference

δ TVC deflection angle

I_{cg} moment of inertia of the missile about the center of gravity

L_{pg} distance from aerodynamic center of pressure to center of gravity

L_{tg} distance from TVC control to center of gravity

The aerodynamic force acting on a lifting body, in this case the wings and control surfaces of the missile, may be resolved into two components, which are

$$F_{\text{lift}} = C_L \frac{\rho}{2} V_m^2 S \quad (3-6)$$

and

$$F_{\text{drag}} = C_D \frac{\rho}{2} V_m^2 S \quad (3-7)$$

where $(\rho/2)V_m^2$ is the dynamic pressure in N/m^2 .

The lift and drag coefficients are functions of angle of attack (α), and Mach number. Actual values for C_L and C_D must be measured, as they are highly dependent on the airfoil geometry. However, C_L and C_D may be modeled satisfactorily using the following approximations:

$$C_L \cong 0.1\alpha \quad (3-8)$$

$$C_D \cong \frac{2T}{\rho V_{\text{max}} S} (1 + 0.2\alpha^2). \quad (3-9)$$

These coefficients are in reasonable agreement with reference [2] at low angles of attack ($\alpha < 10^\circ$). The only time the missile can expect to exceed 10° angle of attack is during the tip-over phase, when velocity, and therefore lift and

drag forces, are small compared to the thrust force. This is considered an appropriate approximation for the scope of the model under discussion.

A. BOOST PHASE CONTROLLER

The primary objective of the missile control system in the boost phase of flight is to tip the missile over and point the missile in the general direction of the target in minimum time. Therefore, θ , the angle that the missile makes with the horizontal reference, is a logical choice for a control variable. If the force that creates the moment that tips the missile over can be controlled, a general control algorithm can be formulated. This is shown graphically in Figure 6.

At launch, the missile is assumed to be in a vertical position, with the velocity vector pointing straight up, i.e. $\theta = 90^\circ$ and $\gamma = 90^\circ$. In the initial boost phase, it is assumed that the first two terms of equation (3-5) are negligible as compared to the third. Therefore, equation (3-5) may be simplified to

$$\ddot{\theta} = \frac{-TL_{cg} \sin \delta}{I_{cg}}. \quad (3-10)$$

In state space, this can be represented as

$$\begin{bmatrix} \dot{\theta} \\ \ddot{\theta} \end{bmatrix} = \begin{bmatrix} 0 & 1 \\ 0 & 0 \end{bmatrix} \begin{bmatrix} \theta \\ \dot{\theta} \end{bmatrix} + \begin{bmatrix} 0 \\ 1 \end{bmatrix} \left(\frac{-TL_{cg} \sin \delta}{I_{cg}} \right). \quad (3-11)$$

The only term in equation (3-11) that can be used to control θ is δ , the TVC deflection angle. A simple and effective method for controlling missile tip over is to employ the Bang-Bang controller, developed in Chapter II, to drive θ to 0 (horizontal flight) in minimum time, as shown in Figure 7. Thus, the control law is

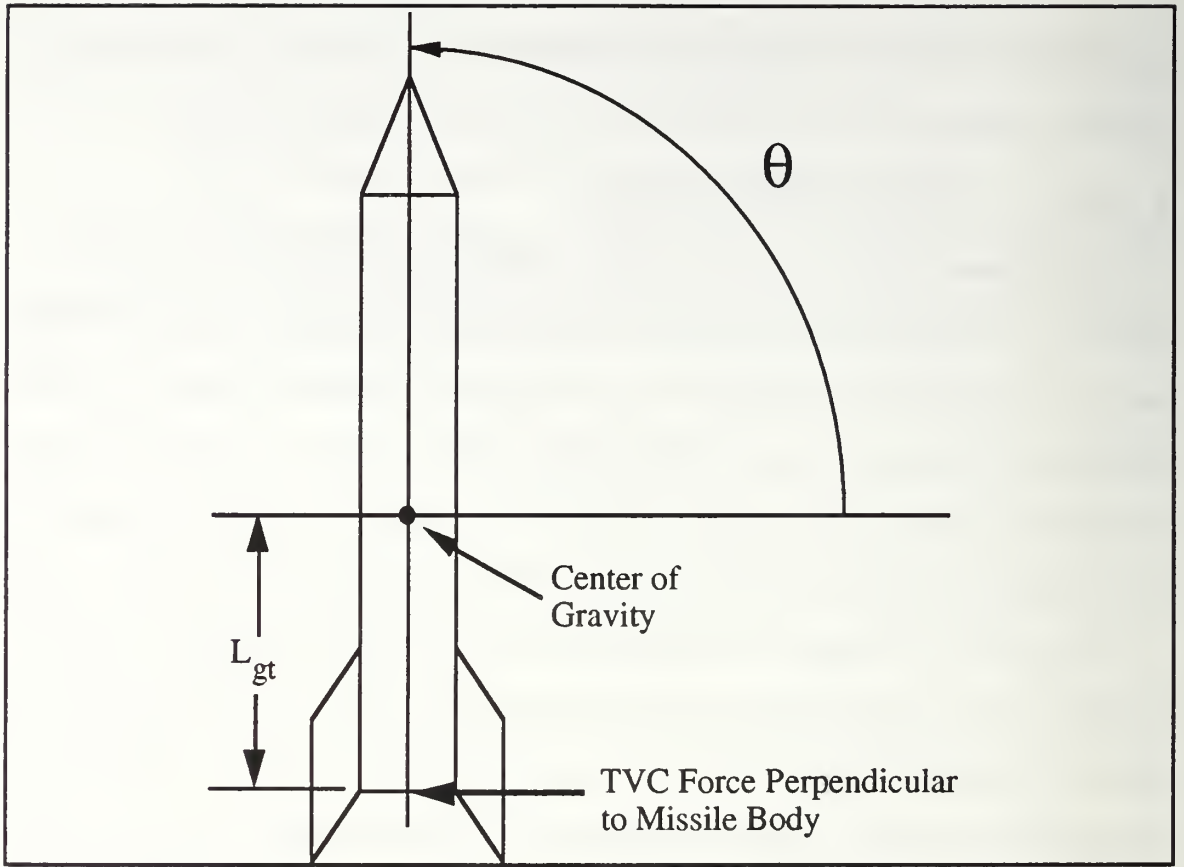


Figure 7. Boost Phase Diagram

$$u(t) = -N \text{sign} \left(\theta(t) + \frac{1}{2N} \dot{\theta}(t) |\dot{\theta}(t)| \right) \quad (3-12)$$

where N is the maximum torque available to rotate the missile and is determined from the relation

$$N = -\frac{TL_{cg}}{I_{cg}} \sin(\delta_{\max}) \quad (3-13)$$

and δ_{\max} is the maximum thrust vector control (TVC) angle available.

This indicates that for minimum tip-over time, $\delta_{\max} = 90^\circ$. However, this may not be desirable since all of the thrust will go to rotate the missile, while

none of the thrust will accelerate the missile downrange. This amounts to the missile 'pin-wheeling' in the air. Therefore, TVC angles of less than 90° should be used. Several TVC angles will be examined to show the tradeoffs involved.

When the missile achieves horizontal orientation (i.e. $\theta=0^\circ$), the control law will continue to switch from $+N$ to $-N$ in an attempt to keep the missile at exactly 0° . This phenomenon is known as 'chattering'. At this point it is no longer desirable to use maximum control effort to correct for small changes in θ . A satisfactory method for removing the chatter from a Bang-Bang controller is to employ linear control in a small region, of width ϵ , about the desired value, as shown in Figure 8.

This adapted Bang-Bang controller can be expressed mathematically as

$$u(t) = \begin{cases} -N \text{sign}\left(\theta(t) + \frac{1}{2N} \dot{\theta}(t) |\dot{\theta}(t)|\right) & \left|\theta(t) + \frac{1}{2N} \dot{\theta}(t) |\dot{\theta}(t)|\right| > \epsilon \\ -\frac{N}{\epsilon} \left(\theta(t) + \frac{1}{2N} \dot{\theta}(t) |\dot{\theta}(t)|\right) & -\epsilon < \theta(t) + \frac{1}{2N} \dot{\theta}(t) |\dot{\theta}(t)| < \epsilon. \end{cases} \quad (3-14)$$

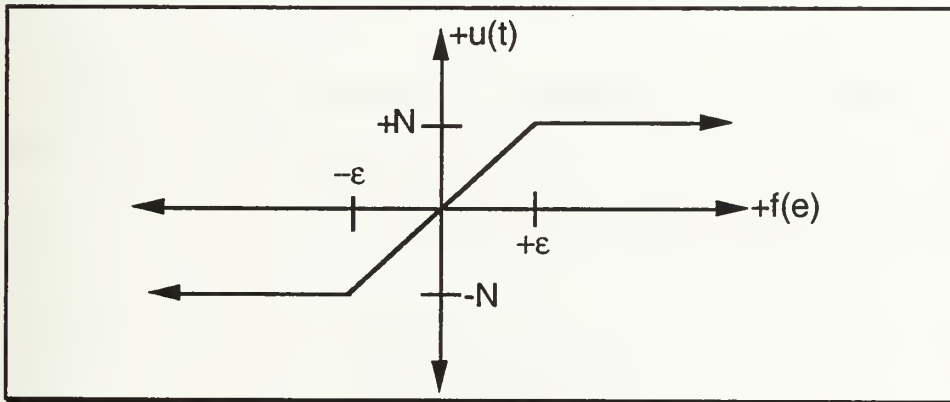


Figure 8. Bang-Bang Control Law with Linear Zone

B. TERMINAL PHASE

1. Missile-Target Geometry

In this section, it will be assumed that the vertically launched surface-to-air missile has completed tip-over, and has settled out to a constant speed and altitude. The start point for the terminal engagement of the target begins with the missile seeker acquiring the target. The geometry of the missile-target engagement is shown in Figure 9.

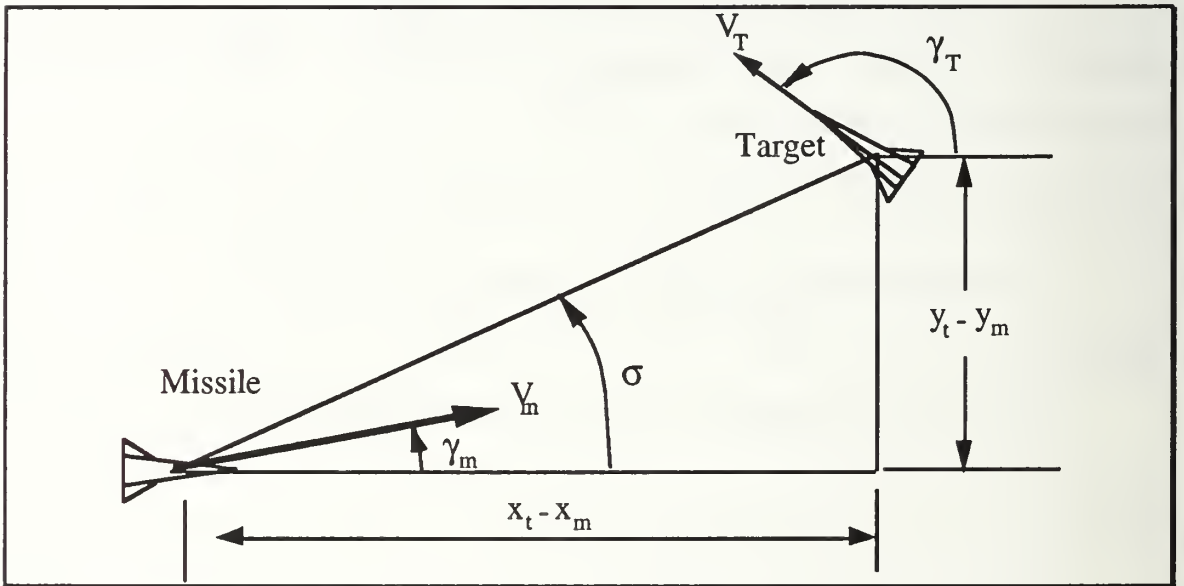


Figure 9. Missile-target geometry

In describing the geometry of the missile-target encounter, several parameters must be calculated. The angle the missile's velocity vector makes with the inertial reference frame is defined as γ :

$$\gamma_m = \tan^{-1} \left(\frac{V_{ym}}{V_{xm}} \right). \quad (3-15a)$$

The magnitude of the missile velocity vector V_m is given by the relation:

$$V_m = \sqrt{V_{xm}^2 + V_{ym}^2} \quad (3-15b)$$

where V_{ym} is the vertical component of the missile velocity vector and V_{xm} is the horizontal component of the missile velocity vector, measured in inertial coordinates.

Similarly, the magnitude of the target velocity vector and angle it makes with the inertial reference is given by

$$V_t = \sqrt{V_{xt}^2 + V_{yt}^2} \quad (3-16a)$$

and

$$\gamma_t = \tan^{-1} \left(\frac{V_{yt}}{V_{xt}} \right). \quad (3-16b)$$

In computing the variables used to calculate the line of sight and its derivatives, it is convenient to describe the relative position, velocity, and acceleration between the target and the missile:

$$X = X_t - X_m \quad (3-17a)$$

$$Y = Y_t - Y_m \quad (3-17b)$$

$$V_x = V_{xt} - V_{xm} \quad (3-17c)$$

$$V_y = V_{yt} - V_{ym} \quad (3-17d)$$

$$A_x = A_{xt} - A_{xm} \quad (3-17e)$$

$$A_y = A_{yt} - A_{ym}. \quad (3-17f)$$

The line of sight between missile and target is given by σ , and is defined as:

$$\sigma = \tan^{-1}\left(\frac{Y}{X}\right) \quad (3-18)$$

where X and Y are the relative cartesian positions as defined by equations (3-17a) and (3-17b). The first and second time derivatives of σ , denoted $\dot{\sigma}$ and $\ddot{\sigma}$, are computed using the relations

$$\dot{\sigma} = \frac{(XV_y - YV_x)}{R^2} \quad (3-19)$$

and

$$\ddot{\sigma} = \frac{XA_y - YA_x}{R^2} - \frac{2(XV_x + YV_y)(XV_y - YV_x)}{R^4}. \quad (3-20)$$

In an actual missile-target engagement, it is very unlikely that the target line of sight rate and acceleration will be measured accurately enough in order to use $\dot{\sigma}$ and $\ddot{\sigma}$ directly in the guidance algorithm. An alternative method is to calculate estimates of $\dot{\sigma}$ and $\ddot{\sigma}$, denoted by $\hat{\dot{\sigma}}$ and $\hat{\ddot{\sigma}}$, based on measured values of σ . This is accomplished through the use of a Luenberger Observer, as shown by the signal flow graph in Figure 10.

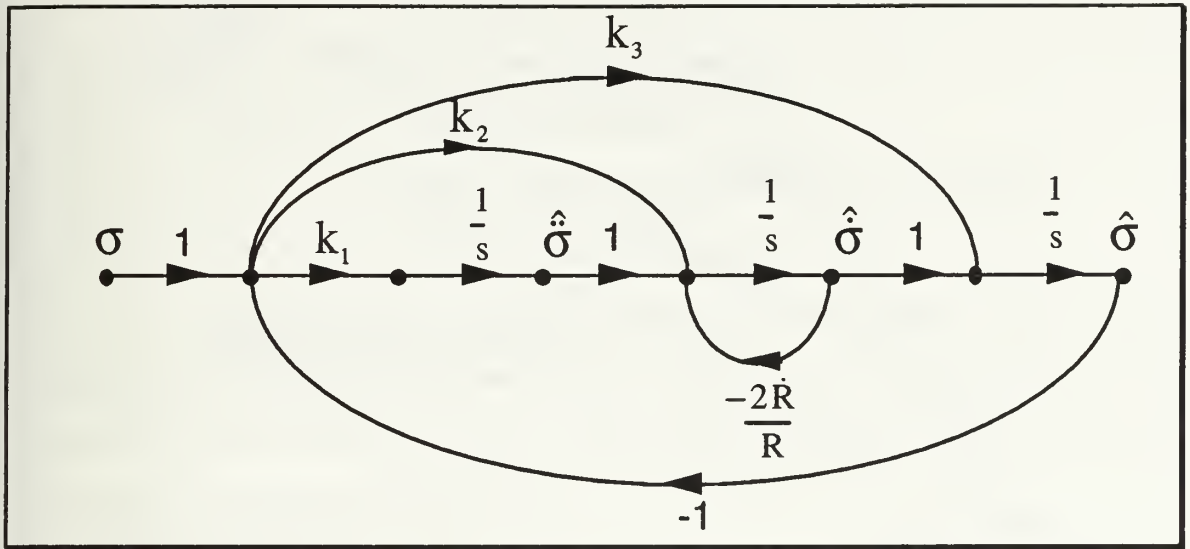


Figure 10. Luenberger Observer for estimating $\dot{\sigma}$ and $\ddot{\sigma}$

This observer can be described in state-space form by the relation

$$\begin{bmatrix} \dot{\hat{\sigma}} \\ \dot{\hat{\dot{\sigma}}} \\ \dot{\hat{\ddot{\sigma}}} \end{bmatrix} = \begin{bmatrix} -k_3 & 1 & 0 \\ -k_2 & \frac{-2\dot{R}}{R} & 1 \\ -k_1 & 0 & 0 \end{bmatrix} \begin{bmatrix} \hat{\sigma} \\ \hat{\dot{\sigma}} \\ \hat{\ddot{\sigma}} \end{bmatrix} + \begin{bmatrix} k_3 \\ k_2 \\ k_1 \end{bmatrix} \sigma \quad (3-21)$$

where R is the range from the missile to the target, \dot{R} is the range rate, and k_1 , k_2 , and k_3 are gains to be determined by the designer in order for the estimated states to closely follow the true states.

2. Missile Guidance Laws

The objective of tactical missile guidance is to keep the line of sight angle, σ , between missile and target constant. This is desirable because if the line of sight remains constant, while the range from missile to target decreases, an intercept will occur, as shown in Figure 11. Two missile guidance laws will be presented: classical proportional navigation and minimum time (Bang-Bang) control.

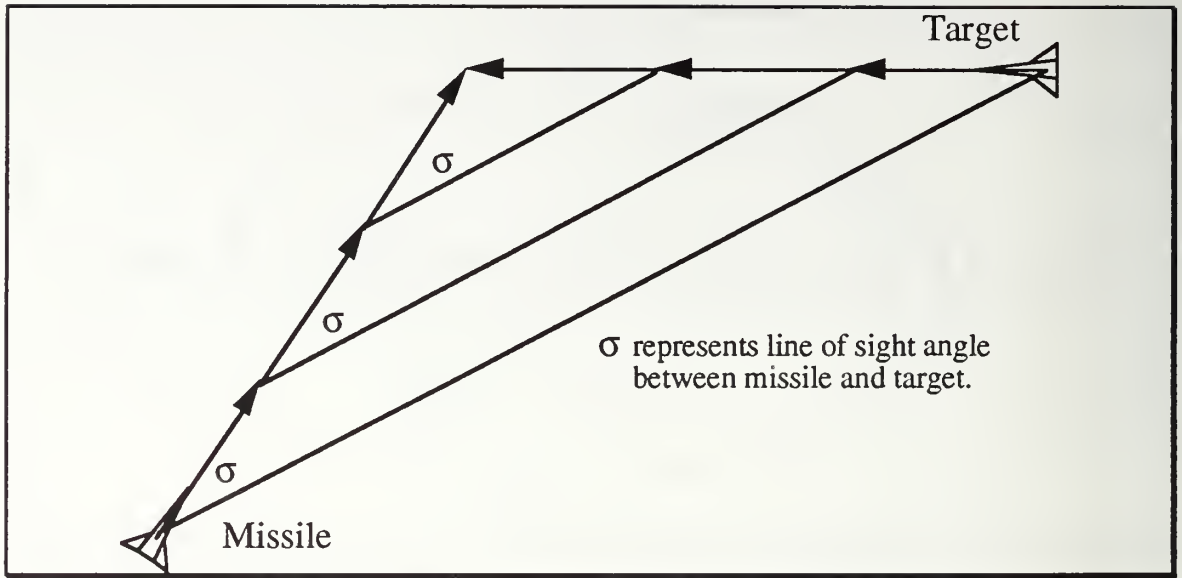


Figure 11. Constant Line-of-Sight Intercept

a. Proportional Navigation Control

The method most often used in controlling homing missiles is known as proportional navigation, where the magnitude of the transverse control force is proportional to the rate of change of the line of sight ($\dot{\sigma}$). Lukenbill [3] conducted research into proportional navigation control and his derivation of the proportional navigation controller is given below.

Figure 12 depicts the basic proportional navigation scheme. Assuming that the seeker head of the missile follows the target, the transverse acceleration perpendicular to the line of sight will equal the acceleration of the R vector in that direction. Mathematically, the acceleration of R is

$$A_R = (\ddot{R} + \omega \times \omega \times R) \hat{i}_R + (2\dot{\omega} \times R + \dot{\omega} \times R) \hat{i}_\theta \quad (3-22)$$

where

R = missile/target line of sight vector

- \dot{R} = closing rate along R
- \ddot{R} = acceleration along R
- ω = angular rate of change of R in inertial space
- A_R = overall acceleration of R.

At this point, a missile acceleration, A_m , equal to the target acceleration, A_t , will make the line of sight parallel to its original direction. As long as \dot{R} remains along R ($\omega=0$) a missile/target intercept is assured. So, the transverse acceleration command is

$$A_t - A_m = \dot{\omega} \times R + 2(\omega \times \dot{R}). \quad (3-23)$$

missile and target cause the line of sight to rotate, resulting in a differential displacement between the missile and the target perpendicular to the range line. Figure 13 depicts this geometry. The proportional navigation guidance law attempts to generate an acceleration command, A_c , perpendicular to the line of sight.

Assume a gyro stabilized seeker head, as in the Sidewinder missile. If there is no torque applied to the gyro, the seeker will not rotate. Assuming the seeker tracks the target, the gyro angle will follow the line of sight. Applying the equation of motion for a gyro stabilized seeker

$$L = I\omega\Omega \tag{3-25}$$

where

- L = applied torque
- ω = spin angular velocity
- I = moment of inertia of the gyroscope
- Ω = rate of precession of the gyroscope.

Applying this to the case when the seeker head tracks the target, Ω is then replaced by the rate at which the gyro is torqued in space. This is simply $\dot{\sigma}$,

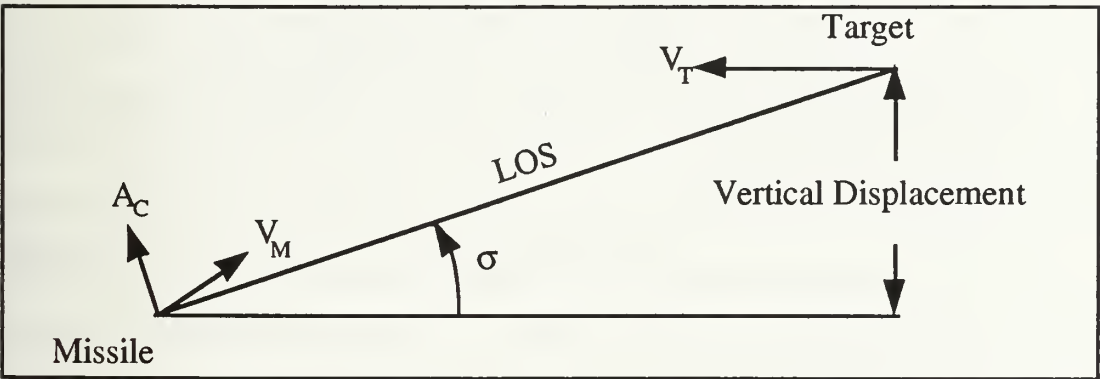


Figure 13. Missile Acceleration Orientation

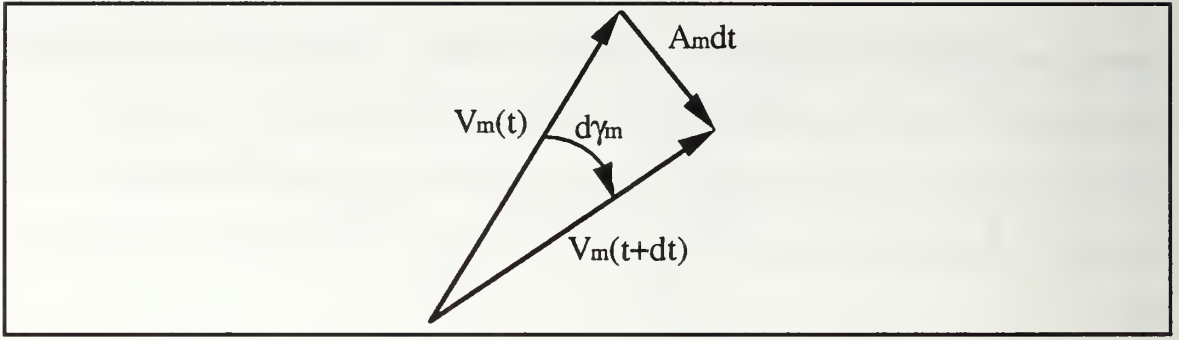


Figure 14. Missile Acceleration Relationship

which is the line of sight rate. Thus, equation (3-25) becomes

$$L = I\omega\dot{\sigma}. \quad (3-26)$$

This torque is in turn applied to the control surface of the missile leading to the relationship

$$A_m = kL = kI\omega\dot{\sigma} \quad (3-27)$$

where k is a constant of proportionality. Referring to Figure 14, a relationship is determined for A_m in terms of the rate of change of the missile flight path angle, $\dot{\gamma}_m$. Given the missile velocity vector at some point in time, $V_m(t)$, and suppose the missile undergoes an acceleration, A_m , during an interval of time, dt . The velocity vector is then displaced and is represented by the vector $V_m(t+dt)$. The angle the vector is traversed is simply $d\gamma_m$, the differential missile flight path angle. For small angles (which are guaranteed by making dt small) the following relationship is obvious:

$$A_m dt = V_m d\gamma_m. \quad (3-28)$$

Dividing equation (3-28) by the time interval, dt , the missile acceleration is defined as

$$A_m = V_m \frac{d\gamma_m}{dt} = V_m \dot{\gamma}_m. \quad (3-29)$$

Combining equations (3-27) and (3-29)

$$V_m \dot{\gamma}_m = kI\omega\dot{\sigma}. \quad (3-30)$$

Dividing through by V_m , the proportional navigation law becomes

$$\dot{\gamma}_m = \left(\frac{kI\omega}{V_m} \right) \dot{\sigma} \quad (3-31)$$

or

$$\dot{\gamma}_m = N\dot{\sigma}. \quad (3-32)$$

Equation (3-32) represents the classical proportional navigation equation where

$\dot{\gamma}_m$ = rate of change of the missile heading

$\dot{\sigma}$ = rate of change of the line of sight

N = proportional navigation ratio.

The navigation ratio determines the sensitivity of the missile system. A high navigation ratio will lead to rather high gains resulting in large missile commands for small changes in the line of sight rate. On the other hand, small values for N will lead to small missile commands for a given $\dot{\sigma}$. Larger navigation ratios are preferred for head on engagements and smaller ones are preferred for tail chase cases. For this research the navigation ratio is taken to be four.

In tactical radar homing missiles using proportional navigation guidance, the seeker provides an effective measurement of the line-of-sight rate, and a Doppler radar provides closing velocity information. [4]

b. Bang-Bang Control Minimizing Line-of-Sight Rate

In this control law, the goal is the same as in proportional navigation control: to drive the line-of-sight rate to zero, or in other words, to keep the line of sight constant.

Mathematically, this control law can be stated as.

$$u(t) = -N \operatorname{sign} \left(\dot{\sigma} + \frac{\ddot{\sigma}|\ddot{\sigma}|}{2N} \right). \quad (3-33)$$

In order to alleviate chattering, a small linear region will be introduced, similar to the boost phase controller:

$$u(t) = \begin{cases} -N \operatorname{sign} \left(\sigma(t) + \frac{1}{2N} \dot{\sigma}(t) |\dot{\sigma}(t)| \right) & \left| \sigma(t) + \frac{1}{2N} \dot{\sigma}(t) |\dot{\sigma}(t)| \right| > \varepsilon \\ -\frac{N}{\varepsilon} \left(\sigma(t) + \frac{1}{2N} \dot{\sigma}(t) |\dot{\sigma}(t)| \right) & -\varepsilon < \sigma(t) + \frac{1}{2N} \dot{\sigma}(t) |\dot{\sigma}(t)| < \varepsilon \end{cases} \quad (3-34)$$

In the next chapter, several simulations will be presented in order to illustrate the effectiveness of the Bang-Bang control algorithms as compared to Proportional Navigation, in both the boost phase and in the terminal phase of the missile flight.

3. Missile Dynamics

The signal flow graphs for the missile dynamics are shown in Figure 15.

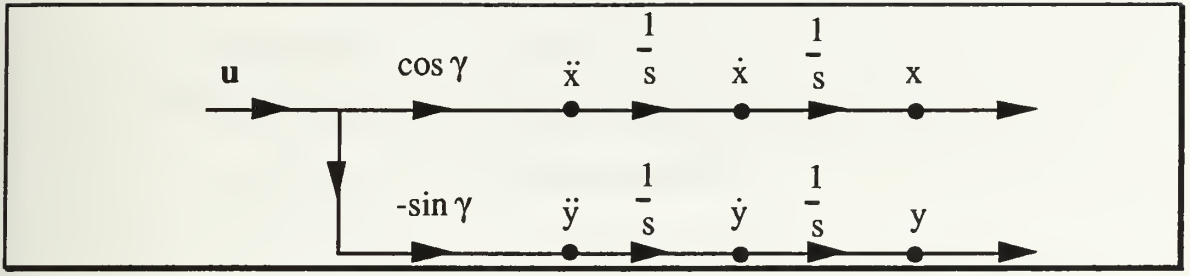


Figure 15. Missile Dynamics

In state-space, these signal flow graphs can be represented as

$$\begin{bmatrix} \dot{x}_m \\ \ddot{x}_m \\ \dot{y}_m \\ \ddot{y}_m \end{bmatrix} = \begin{bmatrix} 0 & 1 & 0 & 0 \\ 0 & 0 & 0 & 0 \\ 0 & 0 & 0 & 1 \\ 0 & 0 & 0 & 0 \end{bmatrix} \begin{bmatrix} x_m \\ \dot{x}_m \\ y_m \\ \dot{y}_m \end{bmatrix} + \begin{bmatrix} 0 & 0 \\ 1 & 0 \\ 0 & 0 \\ 0 & 1 \end{bmatrix} \begin{bmatrix} u \cos \gamma \\ -u \sin \gamma \end{bmatrix}. \quad (3-35)$$

IV. VERTICAL LAUNCH MISSILE BOOST PHASE SIMULATION

A. OVERVIEW

In simulating the boost phase of the vertically launched missile, several assumptions can be made to reduce the complexity of the simulation to a level that won't detract from the concepts being presented:

1. The missile is limited to Mach 4.
2. The missile is limited to 30 g's of acceleration in the transverse and tangential directions combined.
3. The speed of sound in air is constant at 340 m/s.
4. The density of air is constant at 1 Kg/m³.
5. The missile mass remains constant.
6. The lift and drag forces experienced by the missile can be modeled by equations (3-6) through (3-9).

B. MISSILE PARAMETERS

At launch, the following parameters define the state of the missile:

The initial missile parameters are:

$L_m=4.2$ m	missile length
$M=225$ Kg	missile mass
$L_{tg}=2.1$ m	length from center of gravity to tail
$L_{pg}=0.15$ m	length from center of gravity to center of pressure
$S=0.99$ m ²	missile reference lift surface

$T=66800 \text{ N}$	missile thrust
$I_{cg}=2000 \text{ kg m}^2$	missile moment of inertia
$\rho=1. \text{ kg/m}^3$	density of air
$V_{\max}=1460 \text{ m/s}$	max missile velocity

Additionally, the launch point will correspond to inertial reference:

$$\begin{aligned} x(0) &= 0 \text{ m} & y(0) &= 0 \text{ m} \\ V_x(0) &= 0 \text{ m/s} & V_y(0) &= 0 \text{ m/s} \end{aligned}$$

C. CANNISTER EGRESS

It is not possible, nor is it desirable, to have the missile commence its tip-over maneuver until it has egressed from the launch cannister and achieved sufficient distance from the launch platform to minimize hazards to personnel. Thus, the TVC actuators will have a zero degree deflection for the first 0.7 seconds after launch. This will ensure sufficient missile altitude before tip-over begins. At time=0.7 seconds the missile position and velocity are:

$$\begin{aligned} x(0.7) &= 0 \text{ m} & y(0.7) &= 71.8 \text{ m} \\ V_x(0.7) &= 0 \text{ m/s} & V_y(0.7) &= 204.5 \text{ m/s} \end{aligned}$$

D. BOOST SIMULATION AND RESULTS

The simulation was run with four values of the maximum thrust vector control (TVC) angle: 30°, 45°, 60°, and 90°. This was done to illustrate what effect a greater TVC angle will have on the missile trajectory and velocity. Figure 16 shows the missile trajectories for the four cases.

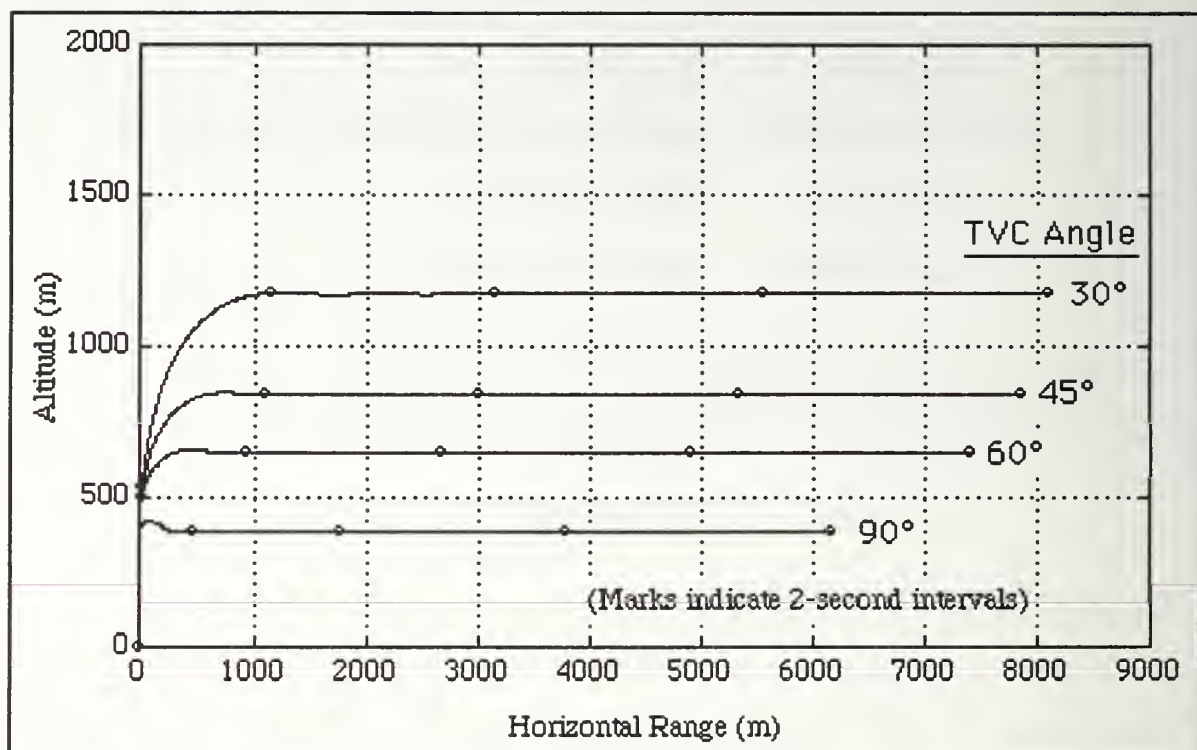


Figure 16. Missile Boost Phase Trajectories

Analysis of the trajectories shows that as the maximum TVC angle is increased, the missile will achieve horizontal flight at lower altitudes than smaller TVC angles. However, at angles greater than 45°, there is a significant reduction in the downrange distance. This may be crucial if the missile is to be fired against a target that is close to the ship at launch. At TVC angles less than 30°, the thrust is directed toward achieving missile altitude to a larger extent than having the missile achieve horizontal flight in minimum time. This may be advantageous if the missile is fired against a high-altitude target, but not against a sea-skimming missile. Another consequence of having a large TVC angle is that much of the thrust is spent rotating the missile to horizontal at the

expense of missile kinetic energy, which results in a longer time for the missile to reach maximum velocity. This is shown graphically in Figure 17.

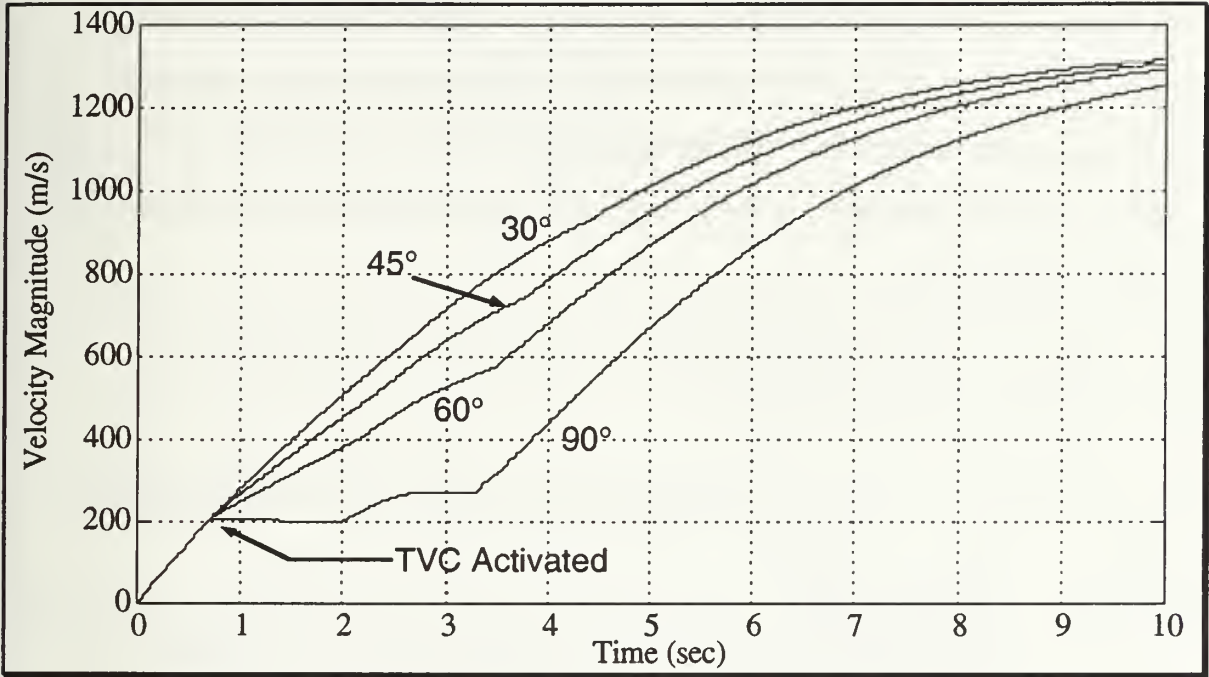


Figure 17. Missile Boost Phase Velocity Magnitude Profiles

At the two highest TVC angles (60° and 90°), the first several seconds are spent turning the missile over while not attaining much forward velocity. As a result of a higher turning rate, higher angles of attack are generated, as shown in Figure 18. This is not desirable because at higher angles of attack, the drag forces that act to slow the missile down increase. Thus, it is advantageous from an aerodynamic point of view to keep the angle of attack as small as possible in order to minimize the drag force acting on the missile.

Figure 19 shows the missile pitch angle as a function of time. It is of interest to note that there is not a great difference between total turning times between the 30° TVC angle and the 90° TVC angle. This is due to the counter-

acting lift and drag forces encountered by the missile, during high TVC angles, that are caused by high angles of attack. This indicates that increasing the maximum TVC angle beyond 45° may achieve a somewhat faster turning time, but at the expense of a great loss of kinetic energy and therefore velocity. This is of peak importance, for without sufficient velocity, a missile has little or no chance of successfully intercepting an incoming target, particularly a maneuvering target.

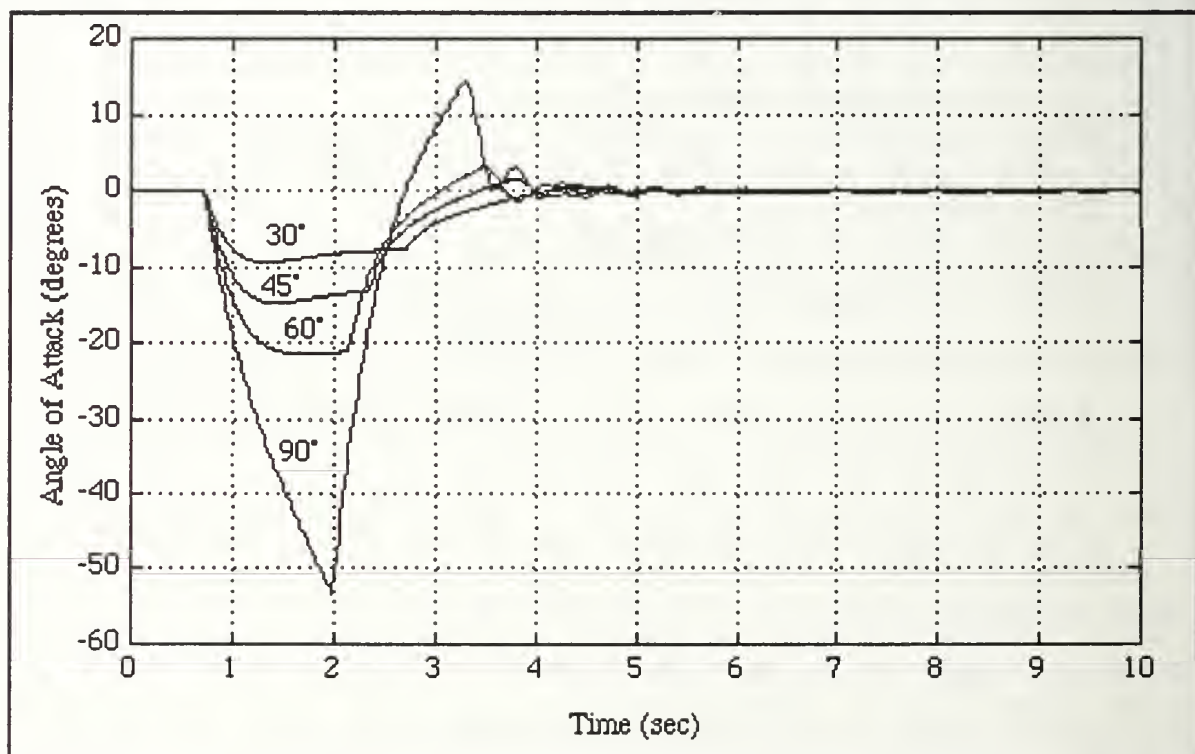


Figure 18. Missile Boost Phase Angle of Attack Profiles

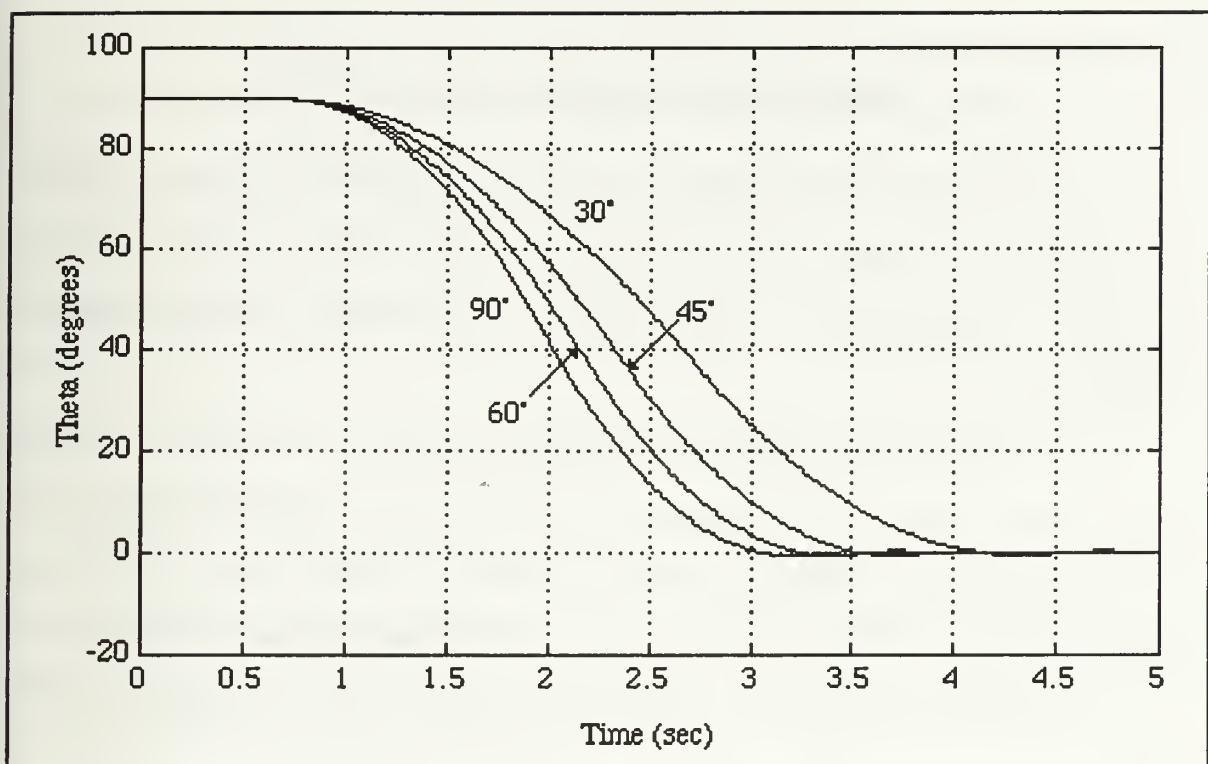


Figure 19. Missile Boost Phase Pitch Angle Profiles

V. TERMINAL PHASE SIMULATIONS

In order to compare the effectiveness of minimum-time 'Bang-Bang' control as compared to proportional navigation control, several missile-target geometries were simulated. Each geometry was run with four control system configurations:

1. proportional navigation using analytical values of line-of-sight rate and acceleration, which shall be referred to as 'analytical proportional navigation';
2. proportional navigation using estimates of line-of-sight rate and acceleration, which shall be referred to as 'estimated proportional navigation';
3. Bang-Bang control using analytical values of line-of-sight rate and acceleration, which shall be referred to as 'analytical Bang-Bang';
4. Bang-Bang control using estimates of line-of-sight rate and acceleration, which shall be referred to as 'estimated Bang-Bang';

A. CASE ONE

In the first set of simulations, the target will be headed directly toward the ship, flying a straight course with no maneuvers. The initial conditions are:

Missile:

$$\begin{array}{ll} x=0; & z=1000 \text{ m;} \\ V_x=680 \text{ m/s (Mach 2)} & V_z=0; \end{array}$$

Target:

$$\begin{array}{ll} x=7000 \text{ m;} & z=30 \text{ m} \\ V_x=-850 \text{ m/s (Mach 2.5);} & V_z=0; \end{array}$$

Figure 20 shows the missile-target geometries using true line-of-sight rate and acceleration. Both proportional navigation and Bang-Bang control was able to hit the target. Note that the trajectory using Bang-Bang control flew a straighter course to the intercept point than the trajectory using proportional navigation control. This indicates that Bang-Bang control is able to guide the missile onto an intercept trajectory faster than the proportional-navigation controller, which is continuously changing the missile flight path in order to intercept the target.

Figures 21 and 22 show control force as a function of time for the proportional navigation controller and the Bang-Bang controller, respectively. The proportional navigation controller required continuous control in order to

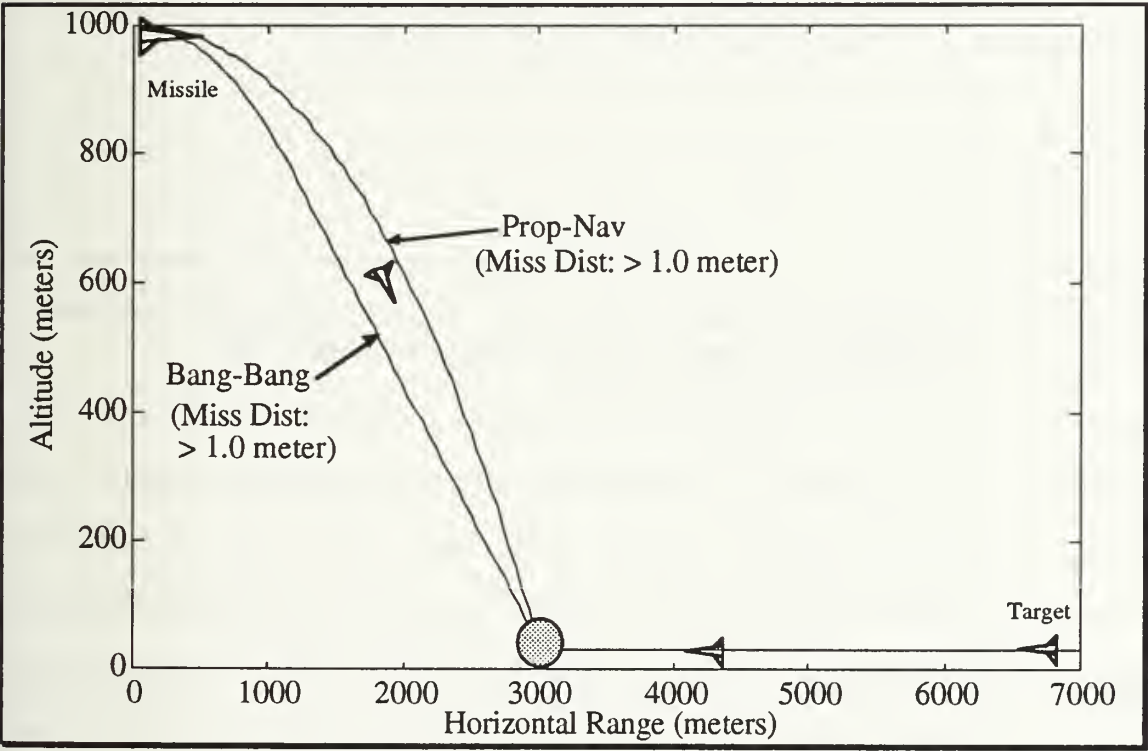


Figure 20. Case One: Missile/Target trajectories using true line of sight rate

correct the missile trajectory enough to enable the missile to intercept the target. It does not leave much reserve control to counter a maneuver away from the missile by the target. Conversely, the Bang-Bang controller applied maximum control effort until the line of sight rate became zero, then shut off. This allows the missile greater flexibility in case the target maneuvers in any direction. If the linear zone were not incorporated into the Bang-Bang controller, however, the controller would have chattered between maximum positive and negative control force instead of shutting off. This would have decreased the missile velocity unnecessarily just when the missile needs maximum kinetic energy for maneuverability.

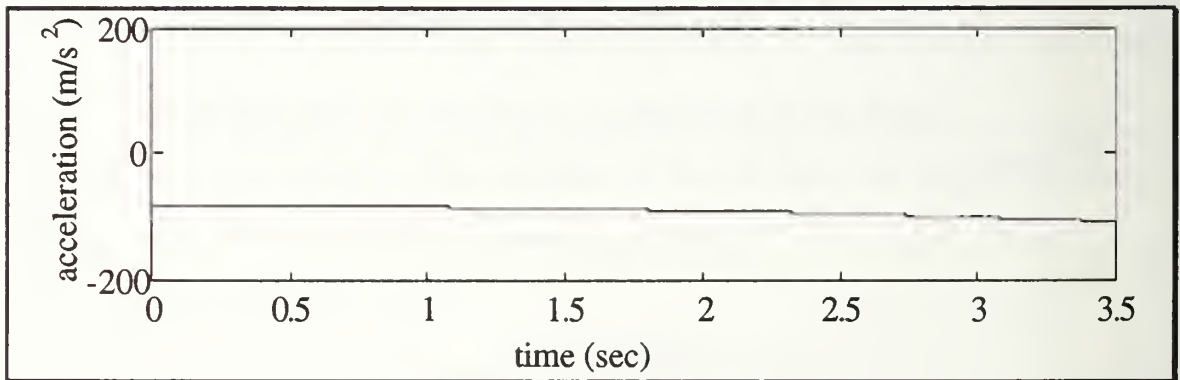


Figure 21. Case One: Control force versus time using proportional navigation control with true line of sight rate

Figure 23 shows the trajectories using estimates of line of sight rate and acceleration. It is apparent here that the proportional navigation controller was not able to react fast enough in order to hit the target. This is due to the delay encountered while the observer filter was not matched up with the analytical values, as shown in Figure 24. By the time the estimated value of line of sight rate and acceleration matched the analytical values, the target was at a point where proportional navigation could not generate enough of a control signal fast

enough to enable target intercept. This illustrates the importance of being able to detect, virtually instantaneously, changes in target velocity and direction. The Bang-Bang controller also experienced the same delay before the proper control was applied, as shown in Figure 25, but since it immediately applied maximum control, the missile was still able to intercept the target.

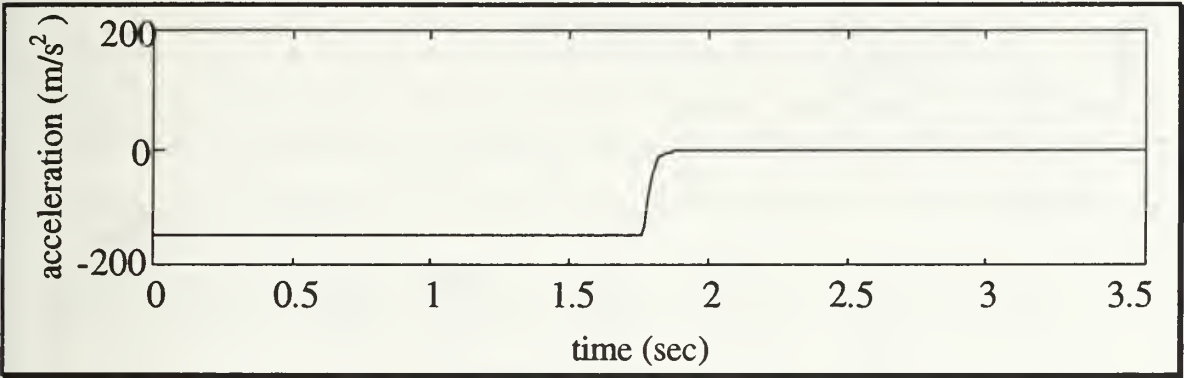


Figure 22. Case One: Control force versus time using Bang-Bang control with true line of sight rate

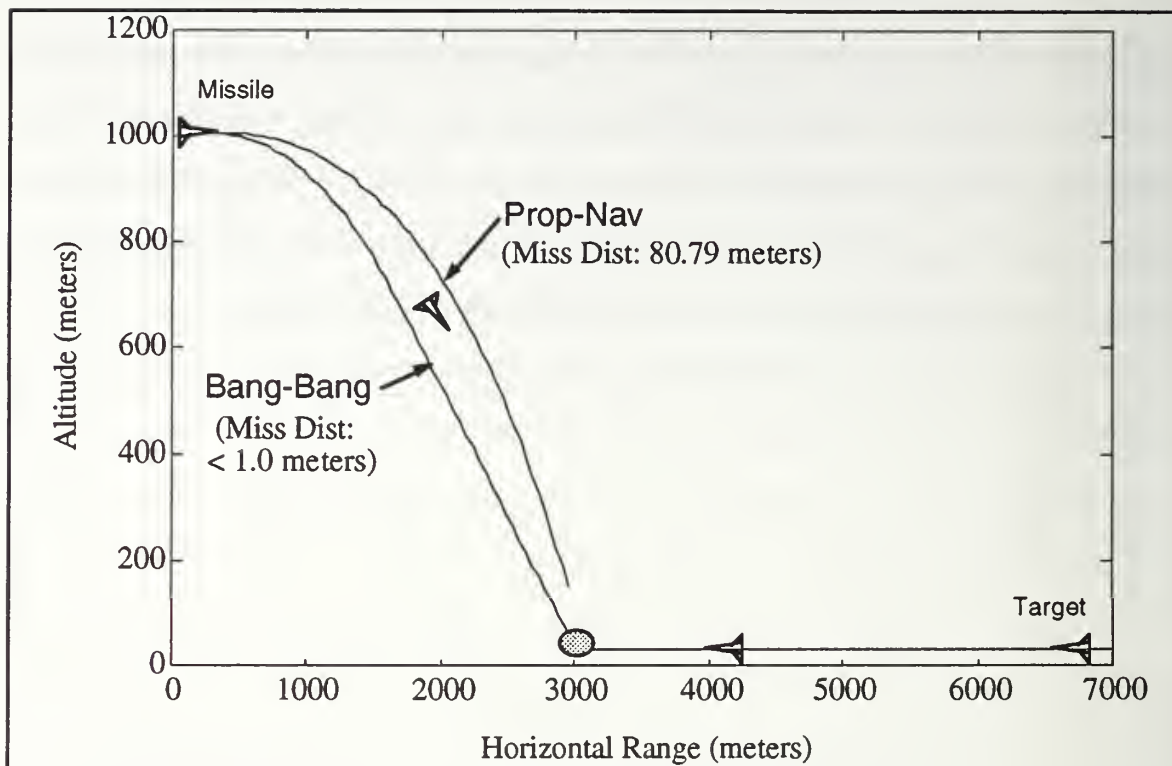


Figure 23. Case One: Missile/Target trajectories using estimated values for line of sight rate

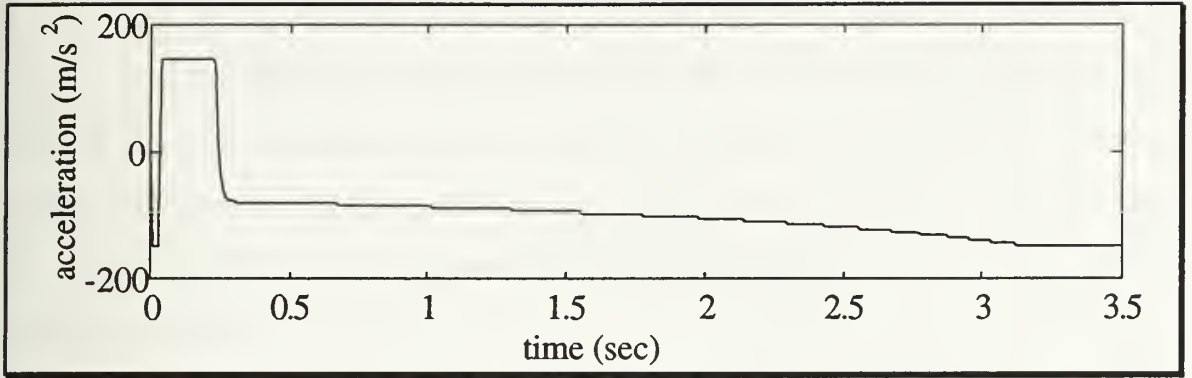


Figure 24. Case One: Control force versus time using proportional navigation control with estimated values for line of sight rate

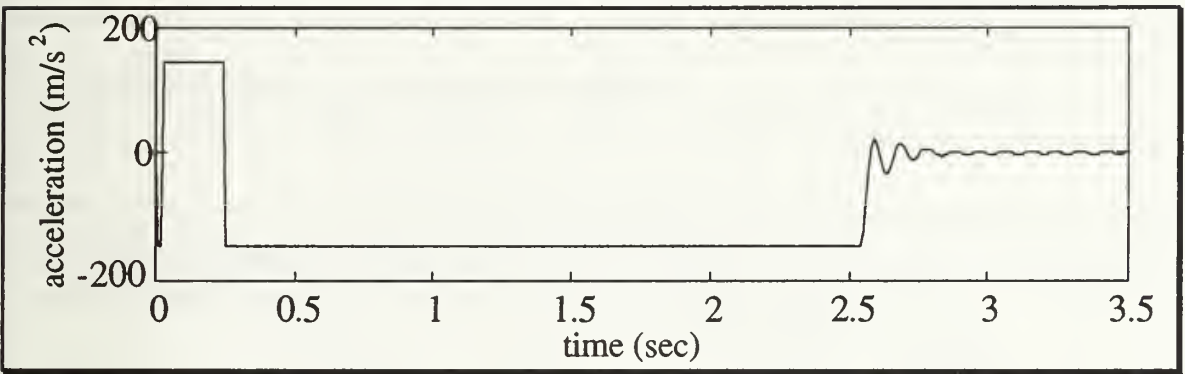


Figure 25. Case One: Control force versus time using Bang-Bang control with estimated values for line of sight rate

Figure 26 compares the trajectories of Bang-Bang control using analytical and estimated values of line of sight rate and acceleration. Because the estimated values took approximately 0.25 seconds to match the analytical values, there is a period at the start of the simulation where the estimated trajectory has positive control applied to it, while the analytic trajectory has negative control applied. After the analytic and estimated values matched up, they both were able to drive the line of sight rate to zero in plenty of time to intercept the target.

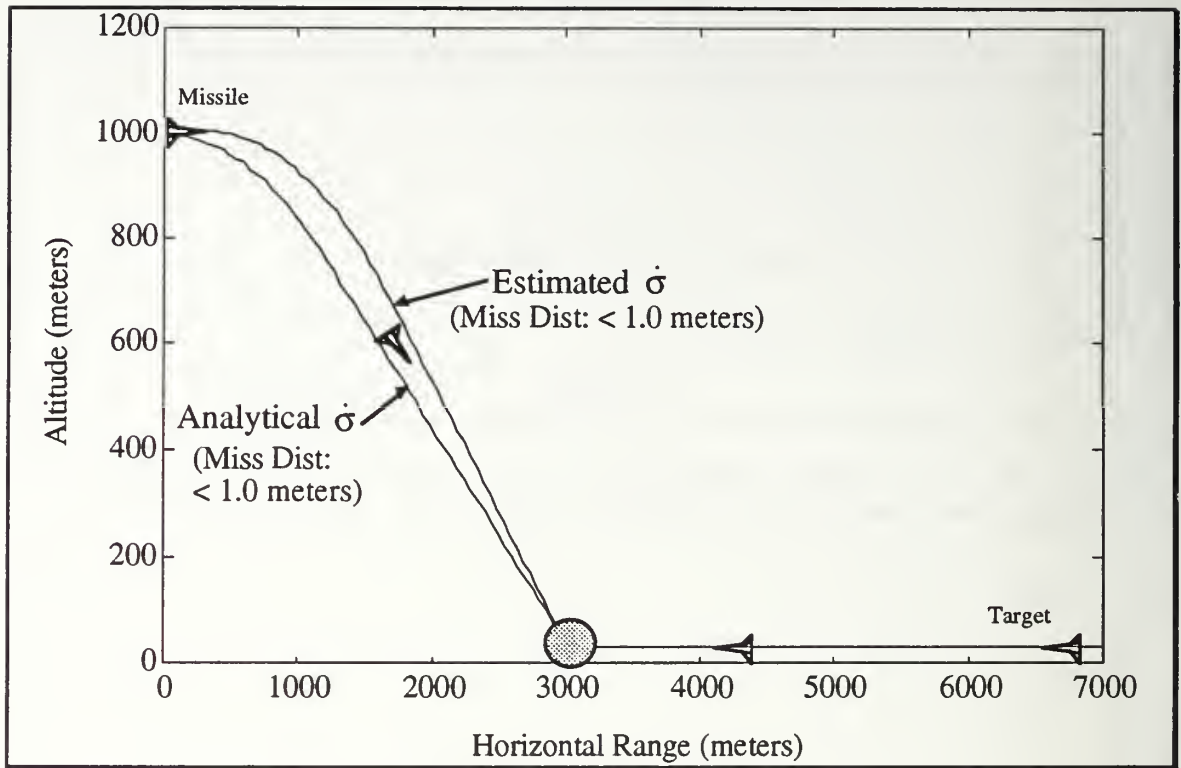


Figure 26. Case One: Missile/Target trajectories using Bang-Bang control, comparing true and estimated values for line of sight rate

B. CASE TWO

In the second set of simulations the target will be headed directly toward the ship, but will initiate a 12 g vertical maneuver at problem start. The initial conditions are:

Missile:

$$x=0;$$

$$z=1000 \text{ m}$$

$$V_x=680 \text{ m/s (Mach 2)}$$

$$V_z=0;$$

Target:

$$x=7000 \text{ m}$$

$$z=30 \text{ m}$$

$$V_x=-850 \text{ m/s (Mach 2.5);}$$

$$V_z=0.$$

Figure 27 shows the simulation results of the analytical proportional navigation and analytical Bang-Bang controllers. The Bang-Bang controlled missile was able to adjust to the 12 g vertical maneuver of the target in order to achieve intercept. The proportional navigation controlled missile was not able to keep up with the high g maneuver of the target, and missed the target by about 80 meters.

Figure 28 shows the control force as a function of time for the analytical proportional navigation controlled missile. Note that the controller did not saturate until well into the simulation. This indicates that if more control had been applied sooner, the missile could have intercepted the target. This is illustrated by Figure 29, which shows the control of the analytical Bang-Bang

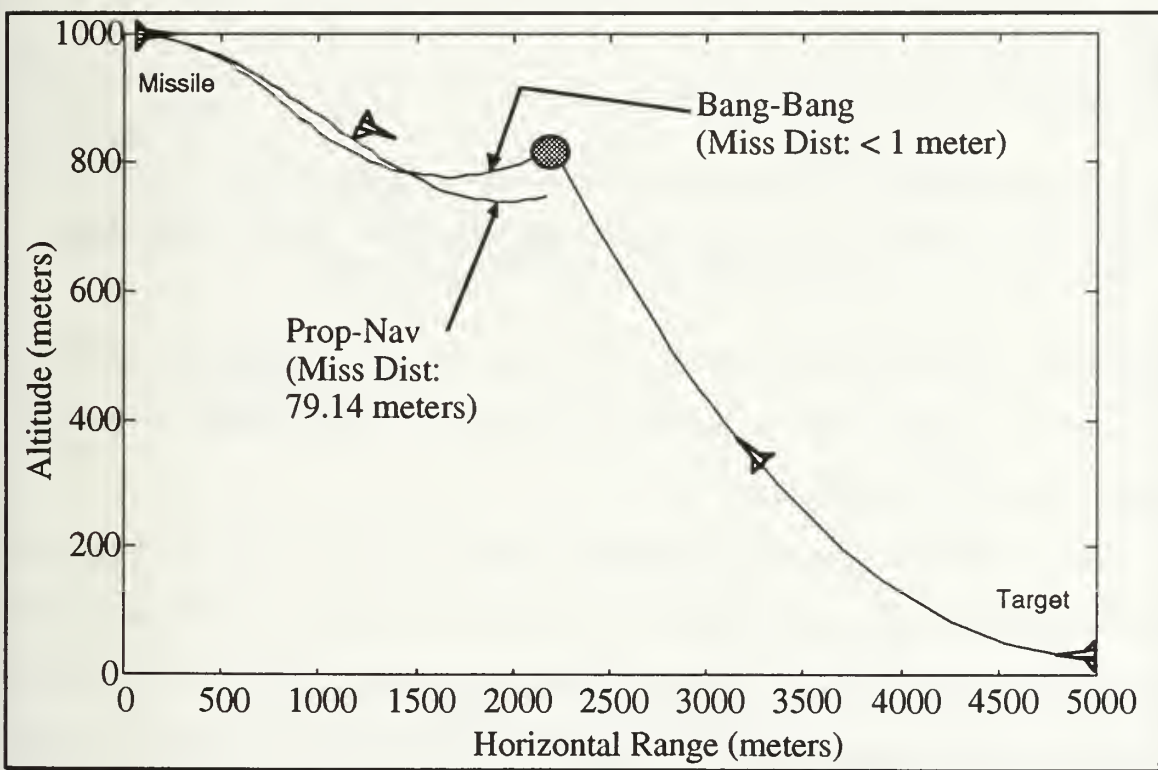


Figure 27. Case Two: Missile/Target trajectories using true line of sight rate

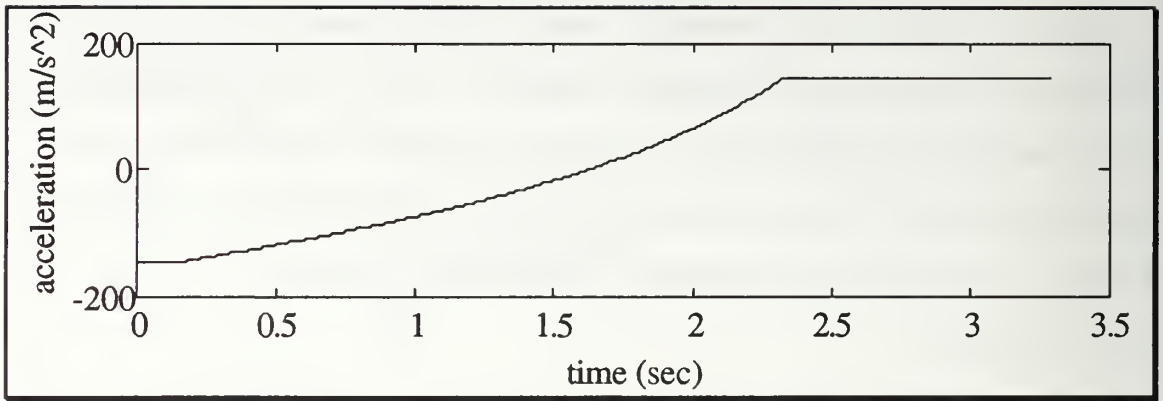


Figure 28. Case Two: Control force versus time using Proportional Navigation control with true line of sight rate

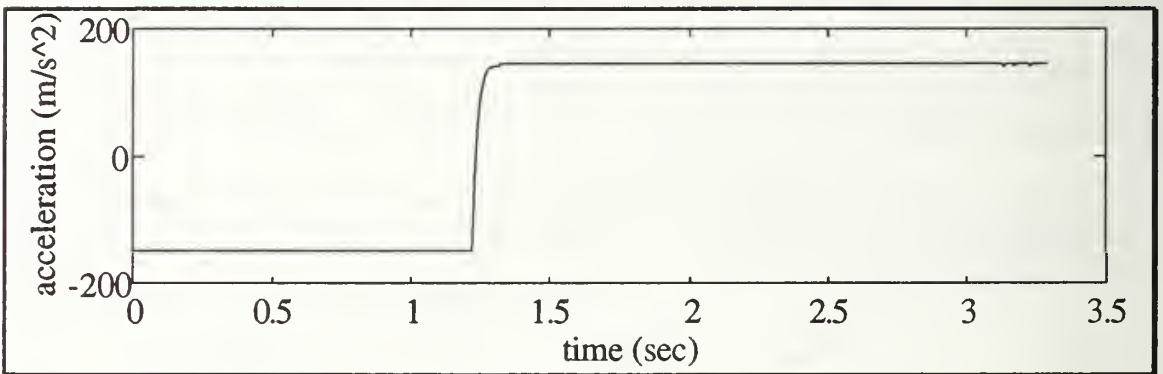


Figure 29. Case Two: Control force versus time using Bang-Bang control with true line of sight rate

controlled missile. Neither controller went to zero as the Bang-Bang controllers of Case One did. This is because the target is maneuvering, constantly changing the line of sight angle.

The simulations using estimated values for line of sight rate and acceleration are shown in Figure 30. As was the case with the analytical expressions, the Bang-Bang controller using estimates was still able to achieve intercept, while the proportional navigation controller missed the target. Note that the miss distance for the proportional navigation controller in Figure 30 is

less than the miss distance achieved with the analytical expressions. This is because the target turned toward the missile, and the delay caused by the observer prevented the missile from beginning to dive after the target as quickly, thus leaving less of an altitude difference when control is applied. If the target were to turn away from the missile, the estimates of line of sight rate and acceleration would be worse than those obtained using analytical values.

Figures 31 and 32 are the control versus time graphs for the estimated proportional navigation controller and the estimated Bang-Bang controller. The delay encountered by both of the controllers is about the same as those encountered in Case One.

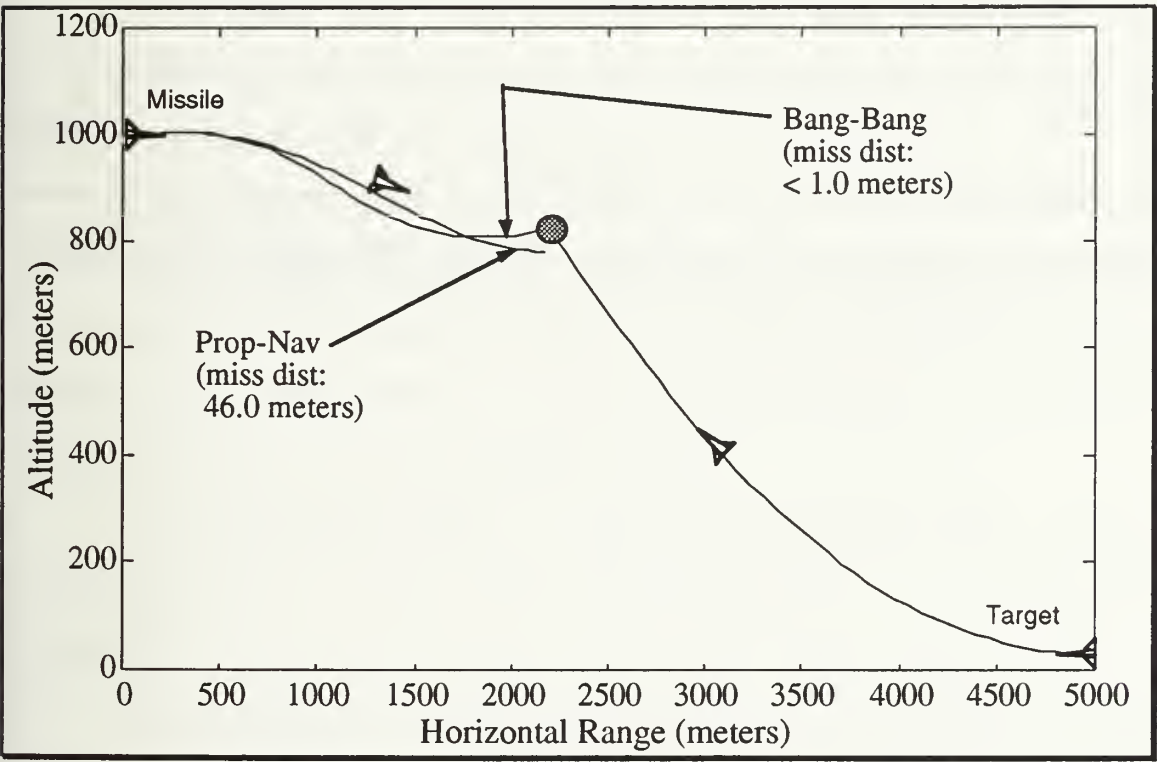


Figure 30. Case Two: Missile/Target trajectories using estimated values for line of sight rate

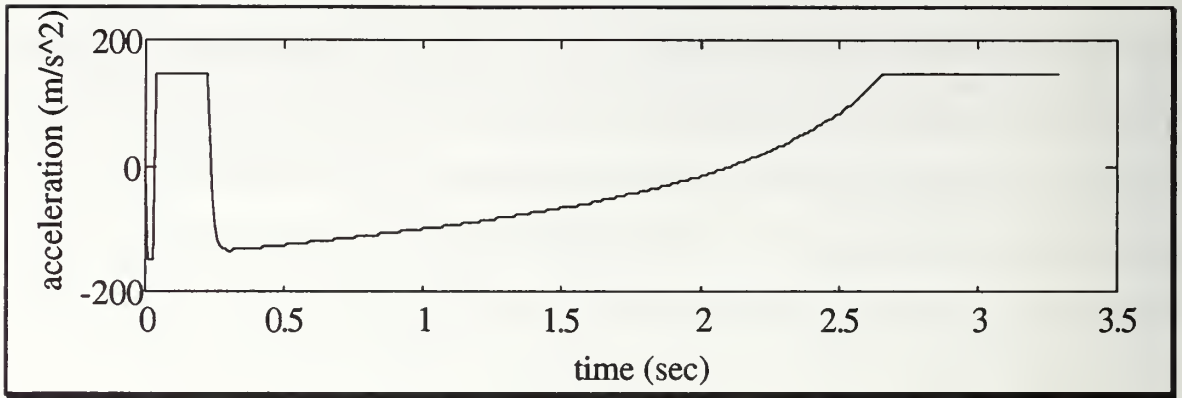


Figure 31. Case Two: Control force versus time using proportional navigation control with estimated values for line of sight rate

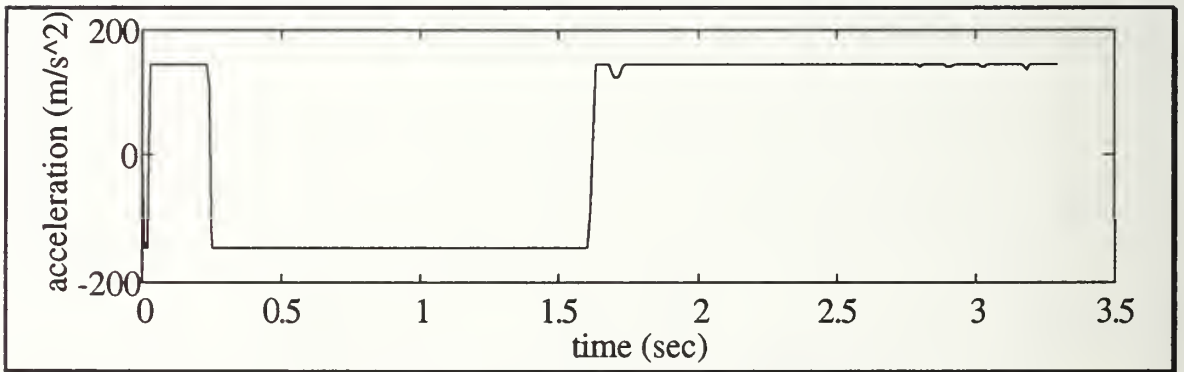


Figure 32. Case Two: Control force versus time using Bang-Bang control with estimated values for line of sight rate

VI. CONCLUSIONS AND RECOMMENDATIONS

This work has shown that the minimum-time (Bang-Bang) controller is an effective algorithm for missile control, in both the boost and terminal phase of tactical missile flight. It is particularly effective when the target has a speed advantage over the missile or when the target is maneuvering.

As is the case with virtually all tactical missiles, the accuracy of the target's measured position, velocity, and acceleration vectors are paramount in accurately predicting the parameters with which the missile is controlled with a Bang-Bang minimum time controller.

Areas for future study will include:

1. Simulating the entire missile flight from launch through intercept. The focus of these studies will be to analyze the effects of missile velocity, tip-over altitude, and target speed advantage on missile performance.
2. Developing more complex models in order to better understand what the effects of a Bang-Bang controller will have on a particular missile system. Such studies will use empirical aerodynamic and physical data for a particular missile, such as SM-II Block IV or Vertically-Launched Sea Sparrow, and will entail developing a 5 or 6 DOF computer model.
3. Investigating the effects of noise on measurement of line of sight and its time derivatives, to the extent of the effect noise has on a Bang-Bang controller.
4. Investigating the effects of plant modelling errors on system sensitivity when using Bang-Bang controllers.

APPENDIX 1- BOOST PHASE MATLAB PROGRAM

% VLS BOOST PHASE MISSILE SIMULATION

% T B MULL

% REVISED 22 APRIL 1992

clear; clg;

% Initial Missile Parameters

Delta=[30 45 60 90];

for j=1:length(Delta)

L_m=3.6; % L_m= missile length in meters

M=227; % M= missile mass in kilograms

L_gt=1.8; % L_gt= length from center of gravity to tail

L_gp=0.15; % L_gp= length from center of gravity to center
% of pressure

S=0.99; % S is lift surface in square meters

T=66800; % T= missile thrust in newtons

Icg=2000; % Icg is the missile moment of inertia (kg m^2)

rho=1.00; % rho is the density of air in kg/m^3

Vmax=340*4; % Vmax is the max missile velocity in m/s

dt=.02; % dt is simulation time step size

delta_max=Delta(j);

% -----

% Initial Conditions

tfinal=10.00; % Final simulation time.

```

kmax=tfinal/dt;           % kmax is number of time increments

time=0.0;                 % initial time

x=0;xdot=0;xddot=0;      % initial missile states (in x)

y=0;ydot=0;yddot=0;      % initial missile states (in y)

                           % (these initial y states correspond to missile
                           % position and velocity after clearing the
                           % cannister)

gamma=90.0;               % gamma is inertial to velocity vector

gammadot=0;              % in degrees (will convert to radians in loop)

theta=90.0;               % theta is inertial to missile head

thetadot=0;

X_theta=[thetadot;theta];

X_x=[xdot;x];

X_y=[ydot;y];

A=[0 0;1 0];             % A and B matrices for determining velocity and
                           % position of x,y, and theta base on acceleration
                           % commands

B=[1;0];

[phi,del]=c2d(A,B,dt);    % converts A,B to discrete for simulation

alpha=theta-gamma;         % alpha is Angle-of-attack

dtr=pi/180;               % converts degrees to radians

V_m(1)=sqrt(X_x(1,1)^2+X_y(1,1)^2); % V_m is missile velocity magnitude

F_drag=0;

F_lift=0;

Cd=0;

```



```

%*****START LOOP*****

for i=1:kmax-1

%****algorithm for determining rudder deflection angle*****
%*****
% test for cannister egress(time<0.6)
if time(i)<0.7
    delta(i)=0;
else
    Theta=X_theta(2,i);
    Thetadot=X_theta(1,i);
    N=T*L_gt/Icg*sin(delta_max*dtr);
    test(i)=Theta+(Thetadot)*abs(Thetadot)/(2*N);
    eps=0.5;

    if abs(test(i))>eps
        delta(i)=delta_max*sign(test(i));
    else
        delta(i)=delta_max/eps*test(i);
    end;
end;

%*****
F_lift(:,i)=0.5*rho*V_m(i)^2*S*0.1*alpha(i);
Cd(i)=(2*T/(M*rho*Vmax^2*S));
F_drag(:,i)=Cd(i)*0.5*rho*V_m(i)^2*S;

```

```

%F_drag(:,i)=0;

xddot(i)=-F_lift(i)/M*sin(gamma(i)*dtr)+T/M*cos(gamma(i)*dtr+delta(i)*dtr)...
-F_drag(:,i)*cos(gamma(i)*dtr);

yddot(i)=F_lift(i)/M*cos(gamma(i)*dtr)+T/M*sin(gamma(i)*dtr+...
delta(i)*dtr)-F_drag(:,i)*sin(gamma(i)*dtr);

thetaddot(i)=-F_lift(i)*L_gp/Icg*cos(alpha(i)*dtr)-T*L_gt*sin(delta(i)*dtr)/Icg;

% -----

X_theta(:,i+1)=phi*X_theta(:,i)+del*thetaddot(i);

X_x(:,i+1)=phi*X_x(:,i)+del*xddot(i);

X_y(:,i+1)=phi*X_y(:,i)+del*yddot(i);

% -----

gamma(i+1)=atan2(X_y(1,i+1),X_x(1,i+1))/dtr;

% X_y=[ydot;y];

alpha(i+1)=X_theta(2,i+1)-gamma(i+1);

delta(i+1)=delta(i);

V_m(i+1)=sqrt(X_x(1,i+1)^2+X_y(1,i+1)^2);

time(i+1)=time(i)+dt;

end;          % END OF LOOP

%*****

eval(['X_x',num2str(j),'=X_x;']);

eval(['X_y',num2str(j),'=X_y;']);

eval(['V_m',num2str(j),'=V_m;']);

eval(['alpha',num2str(j),'=alpha;']);

eval(['X_theta',num2str(j),'=X_theta;']);

delta_max

```

```

vm=V_m(i+1)
X=X_x(2,i+1)
Y=X_y(2,i+1)
Alpha=alpha(i+1)
Theta=X_theta(2,i+1)
end;
Boost1plot2a
save boc3data

clg;
z=length(X_x(2,:));
for k=1:length(Delta)
    eval(['X_x=X_x',num2str(k),';']);
    eval(['X_y=X_y',num2str(k),';']);
    axis([0 9000 0 2000]);
    plot(X_x(2,:),X_y(2,:));grid;
hold on
    if k==1
        plot(X_x(2,1:2/dt:z),X_y(2,1:2/dt:z),'o')
        plot(X_x(2,z),X_y(2,z),'o')
    elseif k==2
        plot(X_x(2,1:2/dt:z),X_y(2,1:2/dt:z),'o')
        plot(X_x(2,z),X_y(2,z),'o')
    else
        plot(X_x(2,1:2/dt:z),X_y(2,1:2/dt:z),'o')

```

```

    plot(X_x(2,z),X_y(2,z),'o')
end;

end;

hold off

title('Missile Boost Phase- Bang-Bang control');
xlabel('Horizontal Range (m)'),ylabel('Altitude (m)');
%text(0.6,0.8,'___ 30° TVC angle','sc')

pause;clg;

axis('normal')

%_____

for k=1:length(Delta)
    eval(['V_m=V_m',num2str(k),';']);
    plot(time,V_m);
    hold on;
end;

hold off

title('V_m versus time');grid;
xlabel('Time (sec)'),ylabel('Velocity (m/s)');

%_____

pause;clg;

for k=length(Delta):-1:1
    eval(['alpha=alpha',num2str(k),';']);
    plot(time,alpha),grid;
    hold on;
end;

```

```

hold off
title('Plot of Alpha versus time')
xlabel('Time (sec)');
ylabel('Angle of Attack (degrees)');
pause;clg;
%_____
axis([0 5 -20 100]);
for k=1:length(Delta)
    eval(['X_theta=X_theta',num2str(k),';']);
    plot(time,X_theta(2,:)),grid;
    hold on;
end;
hold off
title('Plot of Theta versus time')
xlabel('Time (sec)');
ylabel('Theta (degrees)');
axis('normal')

```

APPENDIX 2- TERMINAL PHASE MATLAB PROGRAM

```
% terminal.m
```

```
% TERMINAL MISSILE-TARGET ENGAGEMENT
```

```
% TIM MULL
```

```
% 24 APRIL 1992 1130
```

```
% This model does not take drag or lift into consideration
```

```
% -uses two different methods to compute sigma derivatives:
```

```
% 1. calculates sig_dot, sig_ddot using analytical expressions
```

```
% 2. uses an observer to estimate sighat,sigdothat,sigddothat
```

```
% 3. controls using sigmadothat,sigmaddothat
```

```
% 4. utilized bang bang on sigmadot,sigmaddot with a small linear region
```

```
% in order to alleviate controller chatter once lock has been achieved.
```

```
clear;clg;
```

```
clc;
```

```
disp([' ']);
```

```
for k=1:4
```

```
disp(['Control= ',num2str(k)]);
```

```
control=k;
```

```
dt=0.01;
```

```
%***** Initial Conditions *****
```



```

xm=0; % missile horizontal position in meters
vxm=2*340; % missile horizontal velocity in m/s
axm=0; % missile horizontal acceleration in m/s^2
ym=1000; % missile vertical position in meters
vym=0; % missile vertical velocity in m/s
aym=0; % missile vertical acceleration in m/s^2

xt=5000; % target horizontal position in meters
vxt=-2.5*340; % target horizontal velocity in m/s
axt=0; % target horizontal acceleration in m/s^2
yt=30; % target vertical position in meters
vyt=0; % target vertical velocity in m/s
ayt=0; % target vertical acceleration in m/s^2
time=0;
%-----
%observer stuff
p1=-100;
p2=-100;
p3=-100;
K=conv([1 -p1],conv([1 -p2],[1 -p3]));
k1=K(4);
k2=K(3);
k3=K(2);
X=[0;0;0];
%-----

```

```

for i=1:1200                                %loop 1

    %if rem(i,100)==0

    %clg;

    %subplot(221),plot(xm,ym)

    %subplot(222),plot(time(1:length(U)),U)

    % end;

    gamma(i)=atan2(vym(i),vxm(i));    % gamma is angle of missile velocity
                                       % vector with respect to inertial ref

    Vm(i)=sqrt(vxm(i)^2+vym(i)^2);    % Vm is missile velocity magnitude


X(i)=xt(i)-xm(i);                        % X is relative horizontal position
Y(i)=yt(i)-ym(i);                        % Y is relative vertical position
VX(i)=vxt(i)-vxm(i);                    % VX is relative horizontal velocity
VY(i)=vyt(i)-vym(i);                    % VY is relative vertical velocity
AX(i)=axt(i)-axm(i);                    % AX is relative horizontal acceleration
AY(i)=ayt(i)-aym(i);                    % AY is relative vertical acceleration
R(i)=sqrt(X(i)^2+Y(i)^2);
Rdot(i)=sqrt(VX(i)^2+VY(i)^2);

                                       % sigma,sigmadot,sigmaddot are the line
                                       % of sight between the missile and the
                                       % target, and its 1st 2 time derivatives

%***** NOTE *****
% This simulation is using analytical expressions for sigma *
% sigmadot, and sigmaddot. Since the target's velocity and *
% acceleration cannot be measures directly, a more realistic *

```

```

% approach is to use an observer to estimate sigmadot.hat and *
% sigmaddot.hat.
%*****

sigma(i)=atan2(Y(i),X(i));
sigmadot(i)=(X(i)*VY(i)-Y(i)*VX(i))/R(i)^2;
sigmaddot(i)=(X(i)*AY(i)-Y(i)*AX(i))/R(i)^2...
-2*(X(i)*VX(i)+Y(i)*VY(i))*(X(i)*VY(i)-Y(i)*VX(i))/R(i)^4;
%*****

% 3rd order observer to obtain sigma.dot.hat,sigma.ddot.hat
A=[-k3 1 0
-k2 -2*Rdot(i)/R(i) 1
-k1 0 0];
B=[ k3
k2
k1];
[phi,del]=c2d(A,B,dt);

X(:,i+1)=phi*X(:,i)+del*sigma(i);
sigmadot.hat(i)=X(2,i);
sigmaddot.hat(i)=X(3,i);

%*****

% CONTROL SECTION
%_____

% PROP NAV CONTROL

```

```

if control==1                                % if loop 1
    U(i)=Vm(i)*4*sigmadot(i);
    if abs(U(i))>15*9.81                      % if loop 2
        U(i)=15*9.81*sign(U(i));
    end;                                     % end if loop 2
% _____

% PROP NAV CONTROL based on sigmadothat
elseif control==2                            % if loop 1
    U(i)=Vm(i)*4*sigmadothat(i);
    if abs(U(i))>15*9.81                      % if loop 2
        U(i)=15*9.81*sign(U(i));
    end;                                     % end if loop 2
% _____

elseif control==3                            % if loop 1
%     Bang-Bang control based on sigmadothat, sigmaddothat
N=15*9.81;    % N is maximum normal acceration in Newtons
test(i)=sigmadothat(i)+(sigmaddothat(i)*abs(sigmaddothat(i)))/(2*N);
eps=0.001;
if abs(test(i))>eps                          % if loop 3
    U(i)=N*sign(test(i));
else
    U(i)=N/eps*test(i);
end;                                         % end if loop 3
% _____

elseif control==4

```

```

%      Bang-Bang control based on sigmadot, sigmaddot
N=15*9.81;      % N is maximum normal acceration in Newtons
test(i)=sigmadot(i)+(sigmaddot(i)*abs(sigmaddot(i)))/(2*N);
eps=0.001;
if abs(test(i))>eps
    U(i)=N*sign(test(i));
else
    U(i)=N/eps*test(i);
end;
end;

%_____
if rem(i,50)==0
    disp('working');
end;

% *****update missile states*****

% Let Xmsl=[xm(i)      State space representation of missile states
%      vxm(i)
%      ym(i)
%      vym(i)];
Xmsl(:,i)=[xm(i)
    vxm(i)
    ym(i)
    vym(i)];

Am=[0 1 0 0

```

```

0 0 0 0
0 0 0 1
0 0 0 0];

Bm=[0;-sin(sigma(i));0;cos(sigma(i))]; % control force is perp to sigma!!

[phim,delm]=c2d(Am,Bm,dt); % convert continuous state-space to discrete

% update missile states

Xmsl(:,i+1)=phim*Xmsl(:,i)+delm*U(i);

xm(i+1)=Xmsl(1,i+1);
vxm(i+1)=Xmsl(2,i+1);
axm(i+1)=-sin(sigma(i))*U(i);
ym(i+1)=Xmsl(3,i+1);
vym(i+1)=Xmsl(4,i+1);
aym(i+1)=cos(sigma(i))*U(i);

% *****update target states*****

% Let Xtgt=[xt(i)
%          vxt(i)
%          yt(i)
%          vyt(i)];
Xtgt(:,i)=[xt(i)
           vxt(i)

```



```

        yt(i)
        vyt(i)];

At=[0 1 0 0
    0 0 0 0
    0 0 0 1
    0 0 0 0];
Bt=[0;axt(i);0;ayt(i)];

[phit,delt]=c2d(At,Bt,dt);

Xtgt(:,i+1)=phit*Xtgt(:,i)+delt*1;

xt(i+1)=Xtgt(1,i+1);
vxt(i+1)=Xtgt(2,i+1);
axt(i+1)=axt(i);
yt(i+1)=Xtgt(3,i+1);
vyt(i+1)=Xtgt(4,i+1);
ayt(i+1)=ayt(i);
time(i+1)=time(i)+dt;

%***** check for CPA
X(i+1)=xt(i+1)-xm(i+1);           % X is relative horizontal position
Y(i+1)=yt(i+1)-ym(i+1);           % Y is relative vertical position

```

```
R(i+1)=sqrt(X(i+1)^2+Y(i+1)^2);
```

```
%***** subroutine to interpolate the 2 closest ranges to find CPA
```

```
if R(i+1)>R(i)
```

```
    xms=[ym(i-1:i+1);vym(i-1:i+1);xm(i-1:i+1);vxm(i-1:i+1)];
```

```
    xts=[yt(i-1:i+1);vyt(i-1:i+1);xt(i-1:i+1);vxt(i-1:i+1)];
```

```
    r1 = interp(xms(:,1:2),xts(:,1:2));
```

```
    r2 = interp(xms(:,2:3),xts(:,2:3));
```

```
    Rmin=min([r1 r2]);
```

```
        break;
```

```
end;
```

```
end;
```

```
j=k;
```

```
eval(['xm',num2str(j),' =xm;']);
```

```
eval(['ym',num2str(j),' =ym;']);
```

```
eval(['xt',num2str(j),' =xt;']);
```

```
eval(['yt',num2str(j),' =yt;']);
```

```
eval(['Rmin',num2str(j),' =Rmin;']);
```

```
eval(['U',num2str(j),' =U;']);
```

```
eval(['save data',num2str(j)]);
```

```
end;
```

```
clg;
```

```
clear
```

```
load data1
```

```
save data5 xml yml xt1 yt1
```

```
clear
```

```
load data2
```

```
xm2=xm;
```

```
ym2=ym;
```

```
xt2=xt;
```

```
yt2=yt;
```

```
save data5 xml yml xt1 yt1 xm2 ym2 xt2 yt2
```

```
clear
```

```
load data3
```

```
xm3=xm;
```

```
ym3=ym;
```

```
xt3=xt;
```

```
yt3=yt;
```

```
save data5 xml yml xt1 yt1 xm2 ym2 xt2 yt2 xm3 ym3 xt3 yt3
```

```
clear
```

```
load data4
```

```
xm4=xm;
```

```
ym4=ym;
```

```
xt4=xt;
```

```
yt4=yt;
```

```
save data5 xm1 ym1 xt1 yt1 xm2 ym2 xt2 yt2 xm3 ym3 xt3 yt3 xm4 ym4 xt4
yt4
clear
```

```
%-----
```

```
% This routine takes data computed in terminal.m and samples it every
% 8 data point in order to make the graphs less memory intensive
```

```
clear
load data5
```

```
xm1a=[];ym1a=[];xt1a=[];yt1a=[];xm2a=[];ym2a=[];xm3a=[];ym3a=[];
xm4a=[];ym4a=[];
k=min([length(xm1),length(xm2),length(xm3),length(xm4)]);
for i=1:k
```

```
if rem(i,8)==0
```

```
    xm1a=[xm1a xm1(i)];
    ym1a=[ym1a ym1(i)];
    xt1a=[xt1a xt1(i)];
    yt1a=[yt1a yt1(i)];
    xm2a=[xm2a xm2(i)];
    ym2a=[ym2a ym2(i)];
```

```

        xm3a=[xm3a xm3(i)];
        ym3a=[ym3a ym3(i)];
        xm4a=[xm4a xm4(i)];
        ym4a=[ym4a ym4(i)];

end;

end;

axis([0 5000 0 1200]);

plot(xm1a,ym1a,'-w',xt1a,yt1a,'-w',xm4a,ym4a,'-w')

pause;

plot(xm2a,ym2a,'-w',xt1a,yt1a,'-w',xm3a,ym3a,'-w')


clg;clear


load data1
u1=U;

load data2
u2=U;

load data3
u3=U;

load data4
u4=U;

save control u1 u2 u3 u4

clear

load control

dt=0.01;

```

```
n=min([length(u1),length(u2),length(u3),length(u4)]);  
tfinal=(n-1)*dt;  
time=0.00:dt:tfinal;  
subplot(211),plot(time,u1(1:n),'-w'),title('control=1');  
subplot(212),plot(time,u2(1:n),'-w'),title('control=2');  
pause;clg;  
subplot(211),plot(time,u3(1:n),'-w'),title('control=3');  
subplot(212),plot(time,u4(1:n),'-w'),title('control=4');
```


REFERENCES

- [1] Kirk, D. E., *Optimal Control Theory, an Introduction*, Prentice-Hall, Inc., 1970.
- [2] Blakelock, J. H., *Automatic Control of Aircraft and Missiles*, 2nd Ed., John Wiley & Sons, Inc., 1991.
- [3] Lukenbill, F. C., *A Target/Missile Engagement Scenario Using Classical Proportional Navigation*, M.S. Thesis, Naval Postgraduate School, Monterey, CA, December, 1990.
- [4] Zarchan, P., *Tactical and Strategic Missile Guidance*, American Institute of Aeronautics and Astronautics, Inc., 1990.

INITIAL DISTRIBUTION LIST

	No. Copies
1. Defense Technical Information Center Cameron Station Alexandria, Virginia 22314-6145	2
2. Library, Code 52 Naval Postgraduate School Monterey, California 93943-5100	2
3. Chairman, Code EC Department of Electrical and Computer Engineering Naval Postgraduate School Monterey, CA 93943	1
4. Professor H. A. Titus, Code EC/TS Department of Electrical and Computer Engineering Naval Postgraduate School Monterey, CA 93943	7
5. Professor J. B. Burl, Code EC/BL Department of Electrical and Computer Engineering Naval Postgraduate School Monterey, CA 93943	1
6. Lieutenant T. B. Mull 4 Rose Terrace Grosse Pointe Farms, MI 48236	1

DUDLEY KNOX LIBRARY
NAVAL POSTGRADUATE SCHOOL
MONTEREY CA 93943-5101

GAYLORD S

